$P2X_2$ knockout mice and $P2X_2/P2X_3$ double knockout mice reveal a role for the $P2X_2$ receptor subunit in mediating multiple sensory effects of ATP

Debra A. Cockayne[1], Philip M. Dunn[2], Yu Zhong[1], Weifang Rong[3], Sara G. Hamilton[4], Gillian E. Knight[2], Huai-Zhen Ruan[2], Bei Ma[2], Ping Yip[4], Philip Nunn[1], Stephen B. McMahon[4], Geoffrey Burnstock[2] and Anthony P. D. W. Ford[1]

[1] *Roche Palo Alto, Palo Alto, CA 94304, USA*
[2] *Autonomic Neuroscience Institute, Royal Free and University College Medical School, London NW3 2PF, UK*
[3] *Department of Biomedical Science, University of Sheffield, UK*
[4] *Neurorestoration Group, CARD, Kings College London SE1 9RT, UK*

Extracellular ATP plays a role in nociceptive signalling and sensory regulation of visceral function through ionotropic receptors variably composed of $P2X_2$ and $P2X_3$ subunits. $P2X_2$ and $P2X_3$ subunits can form homomultimeric $P2X_2$, homomultimeric $P2X_3$, or heteromultimeric $P2X_{2/3}$ receptors. However, the relative contribution of these receptor subtypes to afferent functions of ATP *in vivo* is poorly understood. Here we describe null mutant mice lacking the $P2X_2$ receptor subunit ($P2X_2^{-/-}$) and double mutant mice lacking both $P2X_2$ and $P2X_3$ subunits ($P2X_2/P2X_3^{Dbl-/-}$), and compare these with previously characterized $P2X_3^{-/-}$ mice. In patch-clamp studies, nodose, coeliac and superior cervical ganglia (SCG) neurones from wild-type mice responded to ATP with sustained inward currents, while dorsal root ganglia (DRG) neurones gave predominantly transient currents. Sensory neurones from $P2X_2^{-/-}$ mice responded to ATP with only transient inward currents, while sympathetic neurones had barely detectable responses. Neurones from $P2X_2/P2X_3^{Dbl-/-}$ mice had minimal to no response to ATP. These data indicate that P2X receptors on sensory and sympathetic ganglion neurones involve almost exclusively $P2X_2$ and $P2X_3$ subunits. $P2X_2^{-/-}$ and $P2X_2/P2X_3^{Dbl-/-}$ mice had reduced pain-related behaviours in response to intraplantar injection of formalin. Significantly, $P2X_3^{-/-}$, $P2X_2^{-/-}$, and $P2X_2/P2X_3^{Dbl-/-}$ mice had reduced urinary bladder reflexes and decreased pelvic afferent nerve activity in response to bladder distension. No deficits in a wide variety of CNS behavioural tests were observed in $P2X_2^{-/-}$ mice. Taken together, these data extend our findings for $P2X_3^{-/-}$ mice, and reveal an important contribution of heteromeric $P2X_{2/3}$ receptors to nociceptive responses and mechanosensory transduction within the urinary bladder.

(Received 14 April 2005; accepted after revision 15 June 2005; first published online 16 June 2005)
Corresponding author D. A. Cockayne: Roche Palo Alto, 3431 Hillview Avenue, Palo Alto, CA 94304, USA.
Email: debra.cockayne@roche.com

Extracellular ATP communicates physiological signals through the activation of P2X ligand-gated cation channels and P2Y G-protein-coupled receptors. Of the seven P2X receptor subunits ($P2X_1$–$P2X_7$), evidence supports a major role for $P2X_2$ and $P2X_3$ subunits in mediating the primary sensory effects of ATP (Burnstock, 2000). $P2X_3$ is expressed almost exclusively on small-to-medium diameter sensory neurones, while $P2X_2$ is expressed on medium-to-large diameter sensory neurones, and more broadly within the peripheral and central nervous system (Burnstock, 2003). $P2X_2$ and $P2X_3$ subunits can form homomultimeric $P2X_2$, homomultimeric $P2X_3$, or heteromultimeric $P2X_{2/3}$ receptors, each with unique pharmacological properties. $P2X_3$ receptors are rapidly desensitizing, activated by α,β-methylene ATP (α,β-meATP), and antagonized by 2′,3′-*O*-trinitrophenyl-ATP (TNP-ATP); while $P2X_2$ receptors are slowly desensitizing, insensitive to α,β-meATP, and less sensitive to TNP-ATP than $P2X_3$ receptors (IC_{50} 2 μM *versus* 1 nM for $P2X_3$) (Virginio *et al.* 1998). $P2X_{2/3}$ receptors have similar pharmacology to $P2X_3$ receptors, but the slow desensitization kinetics of $P2X_2$ receptors. In dorsal root ganglia (DRG) sensory neurones, $P2X_3$ and $P2X_{2/3}$ receptors are the predominant P2X receptors (Rae *et al.* 1998; Burgard *et al.* 1999), whereas

 DOI: 10.1113/jphysiol.2005.088435

in nodose sensory neurones the effects of ATP appear to be mediated by $P2X_2$ and $P2X_{2/3}$ receptors (Virginio *et al.* 1998; Thomas *et al.* 1998). In contrast, rat and mouse autonomic ganglion neurones appear to express mainly $P2X_2$ receptors (Dunn *et al.* 2001). Whether $P2X_2$, $P2X_3$ and $P2X_{2/3}$ receptors account for all of the effects of ATP on sensory and sympathetic ganglion neurones remains unclear.

Numerous studies have shown that $P2X_3$ and $P2X_{2/3}$ receptors play a crucial role in nociception and mechanosensory transduction (Jarvis, 2003), but few tools have been available to define the relative contribution of these receptors to specific sensory behaviours. Studies using pharmacological agents, such as the $P2X_1$, $P2X_3$ and $P2X_{2/3}$ selective antagonist TNP-ATP (Tsuda *et al.* 1999*a*,*b*; Jarvis *et al.* 2001; Honore *et al.* 2002*b*; Ueno *et al.* 2003), and the $P2X_3$, $P2X_{2/3}$ selective antagonist A-317491 (Jarvis *et al.* 2002; McGaraughty *et al.* 2003; Wu *et al.* 2004), have shown that peripheral and spinal $P2X_3$ and $P2X_{2/3}$ receptors are involved in transmitting persistent, chronic neuropathic and inflammatory pain. $P2X_3$-deficient mice (Cockayne *et al.* 2000; Souslova *et al.* 2000), and animals treated with $P2X_3$-selective antisense (Honore *et al.* 2002*a*; Barclay *et al.* 2002; Inoue *et al.* 2003) or small interfering RNA (siRNA) (Dorn *et al.* 2004) revealed comparable findings. Tsuda *et al.* (2000) further suggested that mechanical allodynia is mediated by $P2X_{2/3}$ receptors located on capsaicin-insensitive neurones, while thermal hyperalgesia and spontaneous nocifensive behaviours are mediated by $P2X_3$ receptors on capsaicin-sensitive neurones. These findings suggested that $P2X_3$ and $P2X_{2/3}$ receptors modulate different nociceptive pathways.

$P2X_3$ receptors also play a role in visceral mechanosensory transduction. In the urinary bladder (Ferguson *et al.* 1997; Vlaskovska *et al.* 2001; Sun & Chai, 2002) and ureter (Knight *et al.* 2002) ATP is released from the urothelium upon distension. Distension leads to increased afferent nerve activity that is mimicked by ATP and α,β-meATP, and attenuated in $P2X_3$-deficient mice (Vlaskovska *et al.* 2001; Rong *et al.* 2002). ATP and α,β-meATP can directly stimulate the micturition reflex in conscious rats, and this is inhibited by TNP-ATP (Pandita & Andersson, 2004). Moreover, $P2X_3$-deficient mice have reduced urinary bladder reflexes (Cockayne *et al.* 2000). Within the gastrointestinal tract, ATP and α,β-meATP excite extrinsic (Kirkup *et al.* 1999; Wynn *et al.* 2003) and intrinsic (Burnstock, 2001; Bertrand & Bornstein, 2002; Bian *et al.* 2003) afferents, and $P2X_3$-deficient mice have impaired peristalsis (Bian *et al.* 2003).

In the present study, we generated $P2X_2^{-/-}$ and $P2X_2/P2X_3^{Dbl-/-}$ mice to characterize further the P2X subunits mediating ATP responses in sensory and autonomic ganglia, and to further assess the role of $P2X_2$ and $P2X_3$ subunits in pain-related behaviours and urinary bladder reflexes. We have compared these findings to $P2X_3^{-/-}$ mice. Our studies confirm an important role for both $P2X_2$ and $P2X_3$ subunits in sensory afferent signalling in multiple physiological systems.

Methods

Generation of $P2X_2^{-/-}$ and $P2X_2/P2X_3^{Dbl-/-}$ mice

The $P2X_2$ gene was cloned from a 12 kb *Eco*R1 fragment derived from a mouse embryonic stem (ES) cell 129Ola BAC genomic library (Genome Systems, St Louis, MO, USA). The $P2X_2$ targeting vector includes a total of 8.0 kb of genomic sequence, a *LoxP*-flanked neomycin-resistance gene (*Neo*), and the *HSV-TK* gene. Homologous recombination between the targeting vector and the wild-type $P2X_2$ allele results in deletion of a 2.6 kb region of the $P2X_2$ gene encompassing exons 2–11, and replacement of this sequence with the *LoxP*-flanked *Neo* gene. A *Not*I linearized targeting vector was electroporated into 129Ola-derived E14-1 ES cells, and clones were selected in 310 μg ml^{-1} active G418 (Invitrogen, Rockville, MD, USA) and 2 μM gancyclovir (Roche Pharmaceuticals). Southern blot analysis using a 5′ flanking region probe identified positive clones with the predicted 12 and 7 kb *Eco*RI fragments diagnostic of the wild-type and mutant $P2X_2$ alleles. Targeted clones were injected into C57BL/6 J (Jackson Laboratory, Bar Harbour, ME, USA) blastocysts and germline transmission of the targeted allele was established by mating the resulting male chimeras to C57BL/6 J females. $P2X_2$ wild-type and mutant lines were generated on a mixed 129Ola × C57BL/6 J genetic background according to the strategy described at the Banbury Conference on Genetic Background in Mice (Silva *et al.* 1997). Briefly, F2 $P2X_2$ homozygous mutant mice were generated by intercrossing F1 agouti heterozygotes. In contrast, F2 wild-type controls were produced by intercrossing F1 agouti wild-type mice and screening for F2 progeny in which the $P2X_2$ locus is homozygous for the 129Ola genetic background (i.e. derives from the genetic background of the ES cell). F2129Ola/129Ola $P2X_2$ wild-type mice were identified using a PCR assay that distinguishes a sequence polymorphism upstream of the $P2X_2$ gene between 129Ola and C57BL/6 J strains. The primers used for this assay were: $P2X_2$ 5′901S, 5′-CCT TCT GAG TGT GAG GAT GAG-3′; and $P2X_2$ 5′1181AS, 5′-CAT ACT TAG CAA CCT GCC TAT C-3′. The assay generated amplicons of 280 and 305 bp for the 129Ola and C57BL/6 J alleles, respectively. F2 $P2X_2$ wild-type mice (129Ola/129Ola at the $P2X_2$ locus), and F2 $P2X_2$ homozygous mutant mice (129Ola × C57BL/6 J) were used to establish homozygous wild-type and mutant breeding colonies. All studies were performed on F3 mice derived from these crosses. For Southern blot genotyping assays, an internal exon 1 probe was used with a *Bgl*II digest (6.7 kb wild-type and 5.0 kb

mutant allele) and an *Eco*RI digest (12 kb wild-type and 7.0 kb mutant allele). In addition, a three-primer PCR assay was used that generated amplicons of 194 and 350 bp for the $P2X_2$ wild-type and mutant alleles, respectively. The primers were as follows: $P2X_2$ EX11288S, 5′-GTG CAG CTG CTC ATT CTG CTT-3′; $P2X_2$ EX2482AS, 5′-CTG CAC GAT GAA GAC GTA CCT-3′; NEO2S, 5′-ACG AGT TCT TCT GAG GGG ATC GGC-3′.

$P2X_2/P2X_3^{Dbl-/-}$ mice were generated by crossing 129Ola × C57BL/6 $P2X_3^{-/-}$ F2 mice (Cockayne *et al.* 2000) to 129Ola × C57BL/6 J $P2X_2^{+/-}$ F2 mice to generate $P2X_2/P2X_3$ compound heterozygotes. Compound heterozygotes were bred to generate homozygous $P2X_2/P2X_3$ double wild-type and double knockout mice. All mice used for studies were derived from subsequently established homozygous breeding pairs, and are designated $P2X_2/P2X_3^{Dbl+/+}$ and $P2X_2/P2X_3^{Dbl-/-}$ mice. The only exceptions are the wild-type controls used for formalin studies on $P2X_2/P2X_3^{Dbl-/-}$, where B6129PF2/J mice from The Jackson Laboratory were used in place of homozygous-derived $P2X_2/P2X_3^{Dbl+/+}$. All animal use procedures were overseen and approved by the Roche Palo Alto Institutional Animal Care and Use Committee, or by the UK Home Office.

Histopathology and immunohistochemistry

For histopathology, organs were fixed in 10% formalin, embedded in paraffin, and sectioned at 5 μm. Sections were stained with haematoxylin and eosin, and examined under a light microscope. For immunohistochemistry, adult mice were killed by CO_2 inhalation. DRG, nodose ganglia, trigeminal ganglia and superior cervical ganglia (SCG) were dissected and immersed in 4% paraformaldehyde and 0.2% saturated picric acid in 0.1 M phosphate-buffered saline (PBS, pH 7.2) for 4 h. Tissues were saturated with 20% sucrose in PBS, after which the ganglia were rapidly frozen, cut into 10 μm sections, and thaw-mounted on poly-L-lysine-coated slides. For immunofluorescence double labelling, sections were incubated in 10% normal horse serum in PBS for 30 min at room temperature, followed by incubation with a rabbit polyclonal antibody against the rat $P2X_2$ receptor subtype (Roche) (1 : 800) in 10% normal horse serum and 0.1% Triton X-100 in PBS overnight. Sections were then incubated with biotinylated donkey anti-rabbit IgG (Jackson ImmunoResearch, West Grove, PA, USA) (1 : 500) for 1 h, extravidin peroxidase (1 : 1500) for 1 h, biotinyl tyramide for 8 min, and Streptavidin fluorescein (1 : 200) for 10 min. A rabbit polyclonal antibody against the $P2X_3$ receptor subtype (Roche) (1 : 400) was applied as a second primary antibody and detected with Cy3-conjugated donkey anti-rabbit IgG (Jackson ImmunoResearch). The sections were washed and mounted in citifluor.

Compounds used

Atropine, ATP, β,γ-methylene ATP (β,γ-meATP), α,β-meATP, carbachol, dimethylphenylpiperazinium (DMPP), histamine, 5-HT, substance P, γ–aminobutyric acid (GABA) and tetrodotoxin (TTX) were obtained from Sigma Chemical Company (Poole, UK). Pyridoxal-5-phosphate-6-azophenyl-2′,4′-disulphonic acid (PPADS) (tetrasodium salt) was supplied by Tocris Cookson Ltd (Bristol, UK). TNP-ATP was obtained from Molecular Probes (Leiden, Netherlands). Stock solutions of drugs were prepared using deionized H_2O and stored frozen. diinosine pentaphosphate (Ip_5I) was prepared by enzymatic degradation of diadenosine pentaphosphate (Ap_5A) (King *et al.* 1999).

Primary cell culture and electrophysiology

Single neurones from DRG, nodose, SCG and coeliac ganglia of 6- to 8-month-old mice were enzymatically isolated as previously described (Zhong *et al.* 1998). Briefly, mice were killed by CO_2 inhalation. Ganglia were rapidly dissected and placed in Leibovitz's L-15 medium (Life Technologies, Paisley, UK). Ganglia were desheathed, cut and incubated in 4 ml Ca^{2+}/Mg^{2+}-free Hanks' balanced salt solution with 10 mM Hepes buffer (pH 7.0) (HBSS) (Life Technologies) containing 1.5 mg ml^{-1} collagenase (Class-II; Worthington Biochemical Corporation, Reading, UK) and 6 mg ml^{-1} bovine serum albumin (Sigma) at 37°C for 40 min. Ganglia were then incubated with 4 ml HBSS containing 1 mg ml^{-1} trypsin (Sigma) at 37°C for 20 min. The solution was replaced with 3 ml of growth medium comprising L-15 medium supplemented with 10% bovine serum, 50 ng ml^{-1} nerve growth factor, 0.2% $NaHCO_3$, 5.5 mg ml^{-1} glucose, 200 IU ml^{-1} penicillin and 200 μg ml^{-1} streptomycin. The ganglia were dissociated into single neurones by gentle trituration. The cells were then centrifuged at 160 *g* for 5 min, resuspended in 1 ml of growth medium, and plated onto 35 mm Petri dishes coated with 10 μg ml^{-1} laminin (Sigma). Cells were maintained at 37°C in a humidified atmosphere containing 5% CO_2, and used between 2 and 48 h after plating.

Whole-cell voltage-clamp recordings were performed at room temperature using an Axopatch 200B amplifier (Axon Instruments, Union City, CA, USA). Membrane potential was held at −60 mV. The external solution contained (mM): 154 NaCl, 4.7 KCl, 1.2 $MgCl_2$, 2.5 $CaCl_2$, 10 Hepes, 5.6 glucose, and the pH was adjusted to 7.4 using NaOH. Recording electrodes (resistance 2–4 MΩ) were filled with an internal solution which contained (mM): 56 citric acid, 3 $MgCl_2$, 10 CsCl, 10 NaCl, 40 Hepes, 0.1 EGTA, 10 tetraethylammonium chloride, and the pH was adjusted to 7.2 using CsOH (total Cs^+ concentration 170 mM). Series resistance compensation of 72–75% was

used in all recordings. The threshold for the minimum detectable response was set as 10 pA. Data were acquired using pCLAMP software (Axon Instruments). Signals were filtered at 2 kHz (−3 dB frequency, Bessel filter, 80 dB decade^{-1}).

For nodose, SCG and coeliac neurones, compounds were applied by gravity flow from independent reservoirs through a 7-barrel manifold comprising fused glass capillaries inserted into a common outlet tube (tip diameter of ∼200 μm) which was placed about 200 μm from the cell (Dunn *et al.* 1996). One barrel was used to apply drug-free solution to enable rapid termination of drug application. Solution exchange measured by changes in open tip current was complete in 200 ms; however, complete exchange of solution around an intact cell was slower ($\leq$1 s). For DRG neurones, drugs were applied through a similar 4-barrel manifold controlled by computer-driven solenoid valves. The exchange of solution around the cell was complete in $\leq$100 ms. The intervals between agonist applications were 2 min for nodose, SCG and coeliac ganglia neurones, and 3.5 min for DRG neurones. These were sufficient to achieve reproducible responses. All drugs were prepared from stock solutions and diluted in extracellular bathing solution to the final concentration. Traces were acquired using Fetchex (pCLAMP software) and plotted using Origin (Microcal, Northampton, MA, USA).

Nociceptive behavioural testing

The effect of a subplantar injection of P2 receptor agonists or 5% formalin was performed as described (Cockayne *et al.* 2000). Mice were injected intradermally in the plantar surface of one hindpaw using a 30 g needle with varying doses of ATP or α,β-meATP in a total volume of 30 μl, or 5% formalin in a total volume of 20 μl. For P2X agonists, the total time spent lifting the treated paw in a 4 min time bin was measured. For formalin testing, the total time spent licking, biting or flinching the treated paw was measured every 5 min between 0 and 30 min. All animals were killed at the end of the study. The investigator was blinded to the identity of all animals.

MiniPsychoscreen behavioural testing

$P2X_2$-deficient mice were evaluated in a MiniPsychoscreen behavioural test battery at Psychogenics, Inc., Tarrytown, NY, USA (see http://www.psychogenics.com/services.shtml for a complete description of the Psychoscreen battery and methods). Male $P2X_2^{+/+}$ and $P2X_2^{-/-}$ mice were shipped to Psychogenics at 10–12 weeks of age, and were singly housed upon receipt. Mice were allowed to habituate to the colony for 2 weeks, and were handled for 3 days during this time. The test battery included home cage observations in the colony, open field, Irwin test, rotorod, grip strength, visual cliff, tail suspension, tail flick, plantar test, elevated plus maze, place recognition y-maze, prepulse inhibition of startle and pentylenetetrazole (PTZ)-induced seizure. The investigator was blinded to the identity of all animals.

Bladder *in vitro* pharmacology

For *in vitro* tissue bath studies, mice were killed and urinary bladders were dissected into a modified Krebs solution. The tissues were viewed under a dissecting microscope, stripped of adhering fat and connective tissue, and cut to give two strips of detrusor muscle, approximately 10 × 2 mm, from each bladder. Detrusor strips were weighed and prepared for isolated organ bath recording using a dissecting microscope. Silk ligatures were applied to each end of the strip; one end was attached to a rigid support and the other end to an FT03C force displacement transducer. Each strip was suspended in a 10 ml organ bath containing gassed (95% O_2 and 5% CO_2) modified Krebs solution of the following composition (mM): 133 NaCl, 4.7 KCl, 16.4 $NaHCO_3$, 0.6 $MgSO_4$, 1.4 NaH_2PO_4, 7.7 glucose and 2.5 $CaCl_2$, pH 7.3. Experiments were performed at 37 ± 1°C. Separate experiments were performed to study electrical field stimulation (EFS) of the parasympathetic nerves and the action of exogenously applied agonists. Mechanical activity was recorded using the software PowerLab Chart for Windows (version 4; ADInstruments, Castle Hill, NSW, Australia). An initial load of 1 g was applied to the detrusor strips, which were then allowed to equilibrate for not less than 45 min prior to the start of the experiment. The contraction due to a standard concentration of KCl (120 mM) was noted at the end of each experiment. All compounds were prepared from stock solutions and added to the organ bath (volume, 100 μl) to produce the final concentration.

Frequency–response curves to EFS were constructed for detrusor strips (100 V, 0.3 ms, 0.5–32 Hz, 15 s stimulation every 5 min) in the absence of antagonists, and then in the presence of either PPADS (30 μM, one detrusor strip from each bladder) or atropine (1 μM, one detrusor strip from each bladder). The frequency–response curves were then repeated in the presence of both PPADS (30 μM) and atropine (1 μM). All antagonists were incubated for 20 min. The curves were finally repeated in the presence of tetrodotoxin (TTX, 1 μM for 20 min). Detrusor responses to EFS are expressed as means ± S.E.M. of the percentage maximum control response for n = 5–6 determinations.

Non-cumulative concentration–response curves were constructed for various agonists including carbachol (0.01–300 μM, n = 5–11), β,γ-meATP (0.1–300 μM, n = 5–7), and ATP (0.1 μM–1 mM, n = 5–6), and contractile responses are expressed as means ± S.E.M.

of the percentage of the KCl (120 mM) contraction for n determinations. The time interval between application of β,γ-meATP and ATP was 15–20 min to avoid desensitization. Since the concentration–response curves to these agonists did not reach a maximum, it was not possible to calculate pD2 values ($-\log EC_{50}$ concentration). Contractile responses to single concentrations of substance P (0.3 μM, $n = 6$–18), 5-HT (100 μM, $n = 4$–17), and histamine (100 μM, $n = 4$–16) were also determined, and are expressed as means ± S.E.M. of the milligrams of tension developed for n determinations.

For *in vitro* pharmacology, statistical significance between individual groups of mice was tested by a two-way analysis of variance (ANOVA) followed by a *post-hoc* test. Statistical significance between single concentrations of substance P, 5–HT, and histamine for individual groups of mice was tested using a one-way ANOVA followed by Bonferroni's *post-hoc* analysis.

Mouse cystometry

Mice were anaesthetized with urethane, and transurethral closed cystometry was conducted as previously described (Dmitrieva *et al.* 1997; Cockayne *et al.* 2000). The bladder was cannulated transurethrally with a PE-10 polypropylene catheter. A ventral midline laparotomy was performed to confirm complete bladder emptying. Each cystometrogram consisted of slowly filling the bladder with normal saline through the transurethral catheter at a rate of 10 μl min^{-1}, to a total volume of 0.4 ml. The filling rate was controlled by an infusion pump (Harvard Apparatus, Holliston, MA, USA), and the pressure associated with filling was recorded via a pressure transducer using PowerLab (ADInstruments). Contractions greater than 20 cm of H_2O were taken as micturition contractions. For each cystometrogram, the volume at which active contractions occurred (micturition threshold) and the number of contractions per cystometrogram were recorded. The investigator was blinded to the identity of all animals.

Bladder afferent nerve recordings

The mouse urinary bladder/pelvic nerve preparation has been previously described in detail (Vlaskovska *et al.* 2001). Briefly, the whole urinary tract attached to the lower vertebrae and surrounding tissues was isolated *en bloc* and superfused in a recording chamber with oxygenated (5% CO_2 and 95% O_2) Krebs solution (mM: 120 NaCl, 5.9 KCl, 1.2 NaH_2PO_4, 1.2 $MgSO_4$, 15.4 $NaHCO_3$, 2.5 $CaCl_2$, and 11.5 glucose) at ~26°C. The bladder was catheterized through the urethra and connected to a syringe-type infusion pump (sp210iw; World Precision Instruments, Sarasota, FL, USA) for intraluminal infusion with Krebs (0.1 ml min^{-1}). Another double-lumen catheter was inserted into the bladder through a small cut on the bladder dome for measurement of intraluminal pressure and for drainage. Both catheters were secured in place with fine sutures.

With the aid of a dissecting microscope, the pelvic nerve exiting the vertebrae was dissected. Normally, 3–4 nerve branches could be identified at this location and the finest branch was recorded with a suction glass electrode (tip diameter, ~50 μm). The electrode was connected to a NeuroLog head stage (NL 100; Digitimer, UK) and an AC amplifier (NL 104; Digitimer, UK). Signals were amplified (×10 000), filtered (band-pass 200–4000 Hz), and acquired by a computer (sampling frequency 20 000 Hz) with a power 1401 A/D interface and Spike2 software (Cambridge Electronic Design, Cambridge, UK). The nerve activity was counted and plotted as rate histogram.

Following a 60 min stabilization period, repeated ramp distensions (0.1 ml min^{-1}, up to 50 mmHg) were performed at intervals of 10–15 min. The afferent response to distension was initially variable but usually became stabilized after three to five distensions. This stabilized afferent response was used for comparing mechanosensitivity of bladder afferents among different mouse genotypes. The volume and pressure threshold for whole nerves could be determined as the bladder afferents had no spontaneous activity with the bladder empty (e.g. Fig. 10, top panel, NA trace). In many preparations, single-unit activity could be discriminated based on the amplitude and shape of individual waveforms (e.g. Fig. 10, top panel, insert). The afferent activity at different pressure levels was determined using a script for Spike2 and the pressure–response curve was plotted in Graphpad using the Boltzmann sigmoidal equation. Values are expressed as means ± S.E.M., and the statistical significance between genotypes was compared using ANOVA.

Results

Generation and general characterization of $P2X_2^{-/-}$ and $P2X_2/P2X_3^{Dbl-/-}$ mice

Mice carrying a targeted deletion in exons 2–11 of the $P2X_2$ gene were generated using the gene targeting strategy shown in Fig. 1*A* and *B*). $P2X_2$ heterozygous ($P2X_2^{+/-}$) mice developed normally, but when intercrossed produced fewer than expected $P2X_2^{-/-}$ mice (18% *versus* the expected 25% by Mendelian distribution, $n = 794$, $P < 0.0001$, χ^2 test). Although $P2X_2^{-/-}$ mice showed small differences in body weight compared with $P2X_2^{+/+}$ mice (Table 1), these mice were visibly and histopathologically normal for up to 1 year of age. Urinalysis, blood chemistries, and peripheral blood cell

counts were also normal and similar between $P2X_2^{+/+}$ and $P2X_2^{-/-}$ mice (data not shown). Overall, these findings were similar to those observed for $P2X_3^{-/-}$ mice (Table 1 and Cockayne *et al.* 2000).

To further generate mice lacking both the $P2X_2$ and $P2X_3$ receptor subunits, we crossed $P2X_2^{+/-}$ mice to $P2X_3^{-/-}$ mice (Cockayne *et al.* 2000) to generate $P2X_2/P2X_3$ compound heterozygotes. These mice appeared normal, but when intercrossed with each other produced fewer than the expected 1/16 ratio of $P2X_2/P2X_3^{Dbl-/-}$ mice. $P2X_2/P2X_3^{Dbl+/+}$ mice and the few $P2X_2/P2X_3^{Dbl-/-}$ mice that survived (Fig. 1*C*) were used to establish homozygous breeding colonies. Approximately 90% of the $P2X_2/P2X_3^{Dbl-/-}$ pups died between postnatal day 7 and weaning, and they had significantly stunted growth (Table 1), cachexia and dyspnoea. A thorough phenotypic characterization of the nonsurvival phenotype in $P2X_2/P2X_3^{Dbl-/-}$ pups will be presented elsewhere. However, the mortality observed in $P2X_2/P2X_3^{Dbl-/-}$ mice was not due to a failure of maternal nurturing or nursing. Instead, histopathological examination identified suppurative bacterial bronchopneumonia as the cause of death. In addition, all moribund mice that were examined had evidence of distended bladders, enlarged hearts, marked atrophy or hypocellularity of lymphohaematopoietic organs (e.g. bone marrow and thymus), and lack of lymphoid follicle formation in the spleen and mesenteric lymph nodes. Fourteen-day-old mice had elevated neutrophil counts and moderately decreased lymphocyte counts (data not shown). The lymphoid hypocellularity observed in 10- to 14-day-old pups was also observed in 2- to 3-day-old pups, confirming that that these changes were present from birth. In contrast, the ~10% of the $P2X_2/P2X_3^{Dbl-/-}$ mice that survived into adulthood had normal body weights (Table 1), and were histopathologically normal, showing no evidence of gross lymphoid organ deficits at 6 months of age. The mechanism(s) by which surviving mice may have compensated for this phenotype is not entirely clear, and is the subject of continued study. Nevertheless, surviving $P2X_2/P2X_3^{Dbl-/-}$ were used for all subsequent studies described in the present study.

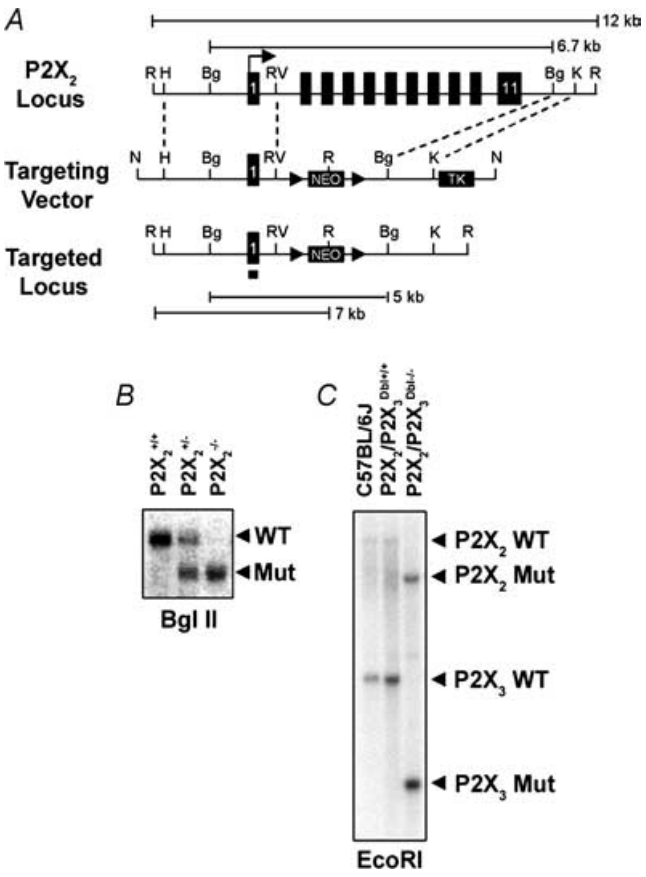

Figure 1. Targeted disruption of the $P2X_2$ gene and generation of $P2X_2^{-/-}$ and $P2X_2/P2X_3^{Dbl-/-}$ mice

A, gene targeting strategy showing the 12 kb genomic fragment of the mouse $P2X_2$ gene used for deletion of exons (filled bars) 2–11. Dashed lines represent the 5′ and 3′ genomic arms of the targeting vector. Position of the *LoxP*-flanked Neo and TK selection markers are indicated. Restriction sites indicated are R, *Eco*RI; H, *Hin*dIII; Bg, *Bgl*II; RV, *Eco*RV; K, *Kpn*I; N, *Not*I. A, *Not*I linearized targeting vector was transfected in 129Ola E14-1 ES cells to generate the targeted $P2X_2$ locus. *B*, *Bgl*II Southern blot used for routine genotyping of $P2X_2^{+/+}$, $P2X_2^{+/-}$ and $P2X_2^{-/-}$ mice using the indicated exon-1-specific probe. $P2X_2/P2X_3$ double knockout mice were generated by conventional backcrossing as described in Methods. *C*, *Eco*R1 Southern blot of C57BL/6 J, $P2X_2/P2X_3^{Dbl+/+}$ and $P2X_2/P2X_3^{Dbl-/-}$ mice probed simultaneously with a $P2X_2$ exon-1-specific probe and a $P2X_3$ 5′ flanking region probe (Cockayne *et al.* 2000). The $P2X_2$ and $P2X_3$ wild-type alleles in the $P2X_2/P2X_3^{Dbl+/+}$ mice are represented by the expected 12 and 3 kb fragments, respectively, and the $P2X_2$ and $P2X_3$ mutant alleles in $P2X_2/P2X_3^{Dbl-/-}$ mice are represented by the expected 7 and 1.5 kb fragments, respectively.

As shown in Fig. 2, immunohistochemical staining of sensory (Fig. 2*A–D*) and sympathetic (Fig. 2*E* and *F*) ganglion neurones confirmed that $P2X_2^{-/-}$ mice lack $P2X_2$ receptor protein (Fig 2*B* and *F*), and that $P2X_2/P2X_3^{Dbl-/-}$ mice lacked protein for both the $P2X_2$ and $P2X_3$ receptor subunits (Fig. 2*D*). Despite the loss of P2X receptor subunits, histological staining indicated no apparent differences in the appearance, density or size distribution of neuronal cell bodies in sensory or autonomic ganglia in these mice (data not shown). There were also no apparent abnormalities in support cells or in the nerve roots around the ganglia (data not shown). These findings are consistent with our previous observations in $P2X_3^{-/-}$ mice (Cockayne *et al.* 2000).

Immunohistochemical and electrophysiological characterization of peripheral ganglion neurones from $P2X_2^{-/-}$ and $P2X_2/P2X_3^{Dbl-/-}$ mice

Peripheral sensory and autonomic ganglion neurones differentially express $P2X_2$ and $P2X_3$ subunits, and show interspecies differences in their distribution. $P2X_2$, $P2X_3$

Table 1. Body weights (g) of $P2X_2$, $P2X_3$ and $P2X_2/P2X_3^{Dbl}$ wild-type (WT) and knockout (KO) mice

Age/sex	Genotype	$P2X_2$	$P2X_3$	$P2X_2/P2X_3^{Dbl}$
2 weeks				
ND	WT	ND	ND	10.2 ± 0.2
ND	KO	ND	ND	$5.3 \pm 0.3^{a,c}$
8 weeks				
M	WT	22.4 ± 0.4	27.4 ± 0.5	25.8 ± 0.4
M	KO	24.7 ± 0.4^{a}	24.3 ± 0.5^{a}	$29.3 \pm 0.7^{a,d}$
F	WT	18.0 ± 0.2	21.9 ± 0.4	21.9 ± 0.4
F	KO	19.1 ± 0.3^{a}	19.8 ± 0.3^{a}	20.3 ± 1.0^{d}
12 weeks				
M	WT	25.0 ± 0.4	27.9 ± 1.0	31.7 ± 1.3
M	KO	27.4 ± 0.5^{b}	24.6 ± 0.5^{a}	31.9 ± 0.5^{d}
F	WT	19.8 ± 0.2	22.5 ± 0.6	24.5 ± 0.7
F	KO	22.4 ± 0.4^{a}	20.3 ± 0.4^{a}	22.8 ± 0.6^{d}
24 weeks				
M	WT	31.5 ± 0.5	36.4 ± 1.5	29.7 ± 1.0
M	KO	32.1 ± 0.6	30.0 ± 0.7^{a}	32.2 ± 0.6^{d}
F	WT	23.2 ± 0.4	25.4 ± 0.7	25.6 ± 0.5
F	KO	23.4 ± 1.3	26.3 ± 0.9	$23.9 \pm 0.6^{b,d}$

Data represent mean ± S.E. of 5–35 mice per group. ND, not determined. $^{a}P < 0.01$, $^{b}P < 0.05$, Unpaired *t* test comparing wild-type *versus* knockout mice. ^{c}Moribund 2-week-old $P2X_2/P2X_3^{Dbl-/-}$ mice. ^{d}Surviving 8-, 12- and 24-week-old $P2X_2/P2X_3^{Dbl-/-}$ mice.

and $P2X_{2/3}$ receptors are dominant in rodent sensory ganglia (North, 2002; Burnstock, 2003), while $P2X_2$ receptors, and possibly a heteromeric receptor containing $P2X_2$, are found in rodent autonomic ganglia (Zhong *et al.* 2000; North, 2002; Calvert, 2004). Consistent with these data, $P2X_2^{+/+}$ and $P2X_2/P2X_3^{Dbl+/+}$ mice had strong $P2X_3$ and $P2X_2$ immunoreactivity in many small-to-medium and small-to-large diameter sensory neurones, respectively, of the DRG, nodosel and trigeminal ganglia, and many neurones showed colocalization of $P2X_2$ and $P2X_3$ subunits (Fig. 2*A* and *C* for DRG, and data not shown). In contrast, in sympathetic SCG neurones of $P2X_2^{+/+}$ mice, most neurones had $P2X_2$ but not $P2X_3$ immunoreactivity (Fig. 2*E*), consistent with reports that $P2X_3$ subunits do not appear to be prevalent in rat and mouse autonomic ganglion neurones (Khakh *et al.* 1995; Zhong *et al.* 2000; North, 2002).

To determine the contribution of $P2X_2$ and $P2X_3$ receptor subunits to ATP-mediated responses in distinct populations of peripheral neurones, we performed whole-cell patch-clamp analysis on dissociated sensory and sympathetic ganglion neurones from wild-type, $P2X_2^{-/-}$ and $P2X_2/P2X_3^{Dbl-/-}$ mice. Results were compared to whole-cell patch-clamp responses from $P2X_3^{-/-}$mice.

In DRG neurones from wild-type mice, ATP and α,β-meATP typically evoked either transient (Fig. 3*Aa*) or sustained (Fig. 3*Ab*) responses, although in a few neurones composite responses with both transient and sustained components were observed (data not shown). For $P2X_2^{+/+}$ mice 81% (17/21) of the neurones tested responded to 100 μM ATP with either a transient (0.28 ± 0.05 nA, $n = 12$) or a sustained (1.22 ± 0.04 nA, $n = 5$) inward current (Table 2). The remaining four neurones failed to respond. In response to 30 μM α,β-meATP, 57% (12/21) of $P2X_2^{+/+}$ DRG neurones responded with a transient response of 0.23 ± 0.05 nA, while 23% (5/21) responded with a sustained response of 0.35 ± 0.1 nA, and four cells failed to respond to this agonist (data not shown). In $P2X_2^{-/-}$ neurones 70% (17/24) of the neurones gave transient currents to 100 μM ATP (0.5 ± 0.09 nA), while 20% (5/24) gave small sustained responses (0.05 ± 0.02 nA) that were significantly different from those seen in the $P2X_2^{+/+}$ DRG neurones (1.22 ± 0.38 nA, $P < 0.05$) (Fig. 3*B* and Table 2). In response to 30 μM α,β-meATP, 65% (15/23) of DRG neurones responded with a transient response of 0.22 ± 0.06 nA, one cell gave a sustained response of 0.02 nA, and the remaining 7/23 cells failed to respond to this agonist (Fig. 3*B*, and data not shown). As previously described (Cockayne *et al.* 2000), all DRG neurones from $P2X_3^{-/-}$ mice failed to respond to α,β-meATP (Fig. 3*Ca*), and although ∼10% of neurones did respond to ATP, these were invariably of the sustained type (Fig. 3*Cb* and Table 2).

In DRG neurones from $P2X_2/P2X_3^{Dbl+/+}$ mice, 56% (10/18) of the neurones tested responded to 100 μM ATP with either transient (0.64 ± 0.38 nA, $n = 7$), or sustained (0.58 ± 0.38 nA, $n = 3$) inward currents (Fig. 3*A* and Table 2). The remaining eight neurones did not respond. These neurones gave the same type of response to 30 μM α,β-meATP (Fig. 3*A*, and data not shown). In contrast, the majority of DRG neurones tested from $P2X_2/P2X_3^{Dbl-/-}$ mice failed to respond to ATP (Fig. 3*Da* and Table 2). No neurones (0/19) tested responded to ATP with transient currents; however, 36% (7/19) of the neurones gave small, sustained currents averaging 0.05 ± 0.02 nA (Fig. 3*Db* and Table 2). No responses to 30 μM α,β-meATP were detected, but all neurones responded to 100 μM GABA (Fig. 3*Da*).

In nodose ganglion neurones from $P2X_2^{+/+}$ mice, 100% (9/9) of the neurones tested responded to 100 μM ATP and α,β-meATP with sustained inward currents averaging 3.8 ± 1 and 1.97 ± 0.6 nA, respectively (Fig. 4*A* top panel, and Table 2). In contrast, 88% (15/17) of $P2X_2^{-/-}$ nodose neurones responded to ATP and α,β-meATP, but with only a rapidly desensitizing response, such that by the end of a 1 s application the response was approximately 15% of the peak amplitude (100 μM ATP, average 0.54 ± 0.12 nA; 100 μM α,β-meATP, average 0.97 ± 0.22 nA) (Fig. 4*A* lower panel, and Table 2). These remaining transient responses were sensitive to the P2X antagonists Ip_5I (Fig. 4*B* and *C*) and TNP-ATP (Fig. 4*C*). In the presence

of 1 μM Ip_5I, the response to 10 μM α,β-meATP was reduced by approximately 50%, while 10 nM TNP-ATP nearly abolished the response. In nodose neurones from $P2X_2/P2X_3^{Dbl+/+}$ mice, 100% (21/21) of the neurones tested responded to 100 μM ATP with a sustained inward current (3.8 ± 0.4 nA) (Fig. 4*D* and Table 2), while in $P2X_2/P2X_3^{Dbl-/-}$ nodose neurones only 26% (7/27) of the neurones tested responded to 100 μM ATP with barely detectable currents (0.04 ± 0.01 nA) (Fig. 4*D* and Table 2). Taken together, these data indicate that $P2X_2$ and $P2X_3$ are the major P2X receptor subunits in nodose and DRG peripheral sensory neurones.

We next measured whole-cell responses to ATP in sympathetic ganglion neurones. Sustained responses to 100 μM ATP were observed in 87% (13/15) of coeliac ganglion neurones from $P2X_2^{+/+}$ mice, with a mean amplitude of 0.48 ± 0.16 nA (Table 2). However, none of these neurones responded to α,β-meATP (data not shown). In coeliac ganglion neurones from $P2X_2^{-/-}$ mice, none of the 14 neurones tested had a detectable response to 100 μM ATP (Table 2). A similar pattern of responses was observed in SCG neurones; 62% (29/47) of $P2X_2^{+/+}$ neurones responded to 100 μM ATP, while only 3% (1/35) of $P2X_2^{-/-}$ neurones had a detectable response (29/47 averaging 0.5 ± 0.3 nA compared with 1/35 with a response of 0.14 nA) (Fig. 5 and Table 2). In SCG neurones from $P2X_2/P2X_3^{Dbl+/+}$ mice, 100 μM ATP evoked a detectable sustained inward current in every neurone tested (17/17), with a mean amplitude of 0.26 ± 0.08 nA (Table 2). Most SCG neurones from $P2X_2/P2X_3^{Dbl-/-}$ mice failed to respond to ATP, and in the 4 of 11 cells that did respond, the inward current was very small (0.016 ± 0.002 nA, $n = 4$) (Table 2).

Nociceptive behavioural responses in $P2X_2^{-/-}$ and $P2X_2/P2X_3^{Dbl-/-}$ mice

Intradermal administration of ATP or α,β-meATP into the hindpaw of rodents elicits a nocifensive behavioural response (Bland-Ward & Humphrey, 1997). $P2X_3$-containing receptors have been shown to mediate part of this response (Bland-Ward & Humphrey, 1997; Tsuda *et al.* 2000; Cockayne *et al.* 2000; Jarvis *et al.* 2001; Honore *et al.* 2002*a*; McGaraughty *et al.* 2003), but the relative contribution of homomeric $P2X_3$ and heteromeric $P2X_{2/3}$ receptors to this behaviour is not entirely clear. When varying doses of ATP (100 and 300 nmol) or α,β-mATP (30, 100 and 300 nmol) were injected into the hindpaw of $P2X_2^{+/+}$ and $P2X_2^{-/-}$ mice, both groups of mice produced similar responses that showed a dose-related increase in the total time spent lifting the treated hindpaw (Fig. 6*A*).

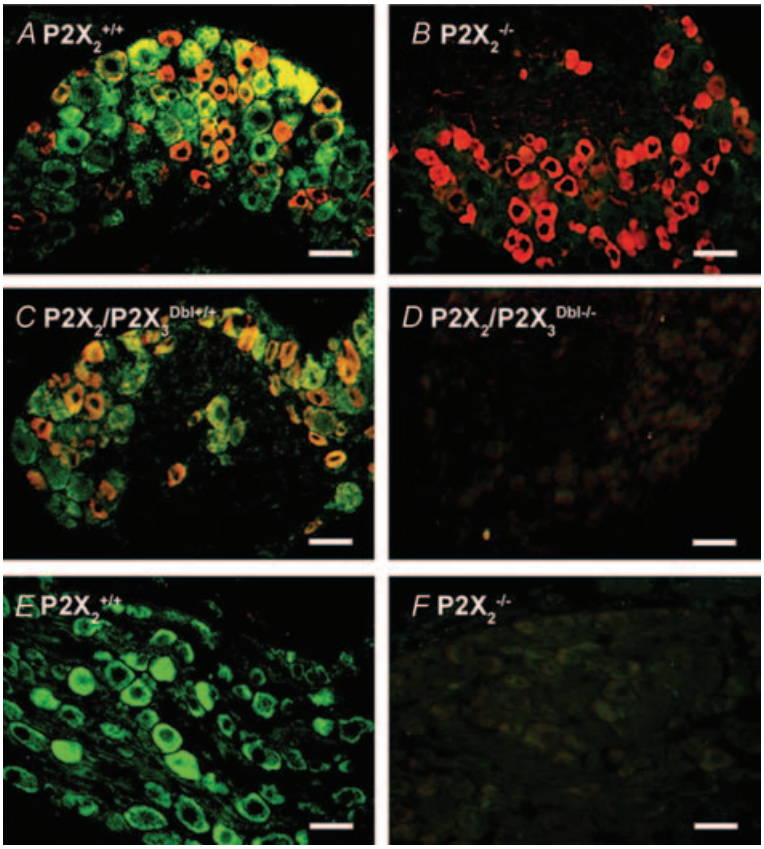

Figure 2. Double immunofluorescence labelling of $P2X_2$ and $P2X_3$ receptors in sensory and sympathetic neurones
A–D, immunofluorescence doubling labelling for $P2X_2$ (green) and $P2X_3$ (red) receptors in transverse sections (10 μm) of DRG (colocalization, yellow) neurones from $P2X_2^{+/+}$ (*A*), $P2X_2^{-/-}$ (*B*), $P2X_2/P2X_3^{Dbl+/+}$ (*C*) and $P2X_2/P2X_3^{Dbl-/-}$ (*D*) mice. $P2X_2$ and $P2X_3$ immunoreactivity was present in small-large and small-medium cells, respectively, in $P2X_2^{+/+}$ (*A*) and $P2X_2/P2X_3^{Dbl+/+}$ (*C*) mice, and many DRG neurones showed colocalization of $P2X_2$ and $P2X_3$ receptors. $P2X_2$ immunoreactivity was absent in $P2X_2^{-/-}$ mice (*B*), while $P2X_3$ immunoreactivity appeared unaltered. Both $P2X_2$ and $P2X_3$ immunoreactivity was absent in $P2X_2/P2X_3^{Dbl-/-}$ mice (*D*). *E* and *F*, immunofluorescence doubling labelling for $P2X_2$ (green) and $P2X_3$ (red) receptors in transverse sections (10 μm) of superior cervical ganglia (SCG) neurones from $P2X_2^{+/+}$ (*E*) and $P2X_2^{-/-}$ (*F*) mice. Many SCG neurones in $P2X_2^{+/+}$ mice showed $P2X_2$ receptor expression (*E*), and this $P2X_2$ immunoreactivity was absent in $P2X_2^{-/-}$ mice (*F*). Specific $P2X_3$ immunoreactivity was not observed in SCG neurones of either $P2X_2^{+/+}$ or $P2X_2^{-/-}$ mice. Scale bars, 50 μM.

$P2X_3$-containing receptors have also been shown to play a role in both the acute (phase I) and persistent inflammatory (phase II) phases of the formalin-induced model of chemical nociception (Cockayne *et al.* 2000; Souslova *et al.* 2000; Jarvis *et al.* 2001; Honore *et al.* 2002*a*; McGaraughty *et al.* 2003). In $P2X_2^{-/-}$ mice, intradermal administration of formalin resulted in a significant attenuation of the late phase formalin response (Fig. 6*B*, 40%, $P < 0.01$), while the early phase was similar to $P2X_2^{+/+}$ mice (Fig. 6*B*). In contrast, $P2X_2/P2X_3^{Dbl-/-}$ mice had significantly attenuated behavioural responses in both phase I (Fig. 6*C*, 26%, $P < 0.01$) and phase II (Fig. 6*C*, 37%, $P < 0.05$) of the formalin response.

We also measured responses to noxious thermal stimuli in $P2X_2^{+/+}$ and $P2X_2^{-/-}$ mice in both the plantar test and the tail-flick test, where infrared light was used as the thermal stimulus. No differences were seen between $P2X_2$ genotypes in these tests of acute thermal nociception (data not shown, MiniPsychoscreen test battery).

Because $P2X_2$ receptors are widely distributed on neurones throughout the peripheral and central nervous system, as well as on non-neuronal cells (Burnstock, 2003), they could conceivably play a role in a broad range of behavioural and neurological functions. To assess the overall integrity of the peripheral and central nervous system, $P2X_2^{-/-}$ mice were profiled in a MiniPsychoscreen battery of behavioural tests. No differences were observed between $P2X_2^{+/+}$ and $P2X_2^{-/-}$ mice in terms of general sensory function and motor coordination as assessed by a neurological evaluation that included the Irwin test, visual cliff, grip strength and rotorod performance (data not shown). $P2X_2^{-/-}$ mice had a tendency toward hyperactivity in the open field test and in home cage behaviours. However, they showed no altered behaviour in depression or anxiety models, including the tail suspension test, open field test and the elevated plus maze (data not shown). $P2X_2^{-/-}$ mice also showed no difference from wild-type controls in response to pentylenetetrazole (PTZ)-induced seizures (data not shown), indicating that there were no gross alterations in the general excitability of the CNS.

Urinary bladder reflexes in $P2X_3^{-/-}$, $P2X_2^{-/-}$ and $P2X_2/P2X_3^{Dbl-/-}$ mice

Cystometry studies were performed on P2X-deficient mice to assess the role of P2X receptor subtypes in sensory afferent signalling within the urinary bladder. Figure 7*A* illustrates representative cystometrograms from $P2X_2^{+/+}$ and $P2X_2^{-/-}$ mice in a urodynamic model of acute cystometry performed under anaesthesia. Distension of the urinary bladder with a fixed infusion rate of saline ($10\,\mu l\,min^{-1}$, 0.4 ml in 40 min) resulted in frequent micturition contractions in $P2X_2^{+/+}$ mice, but markedly reduced contractions in $P2X_2^{-/-}$ mice. The volume threshold for micturition contractions was significantly increased in $P2X_2^{-/-}$ mice (0.28 ± 0.02 ml compared with 0.16 ± 0.02 ml for $P2X_2^{+/+}$ mice, $P < 0.01$) (Fig. 7*B*), while the average number of contractions

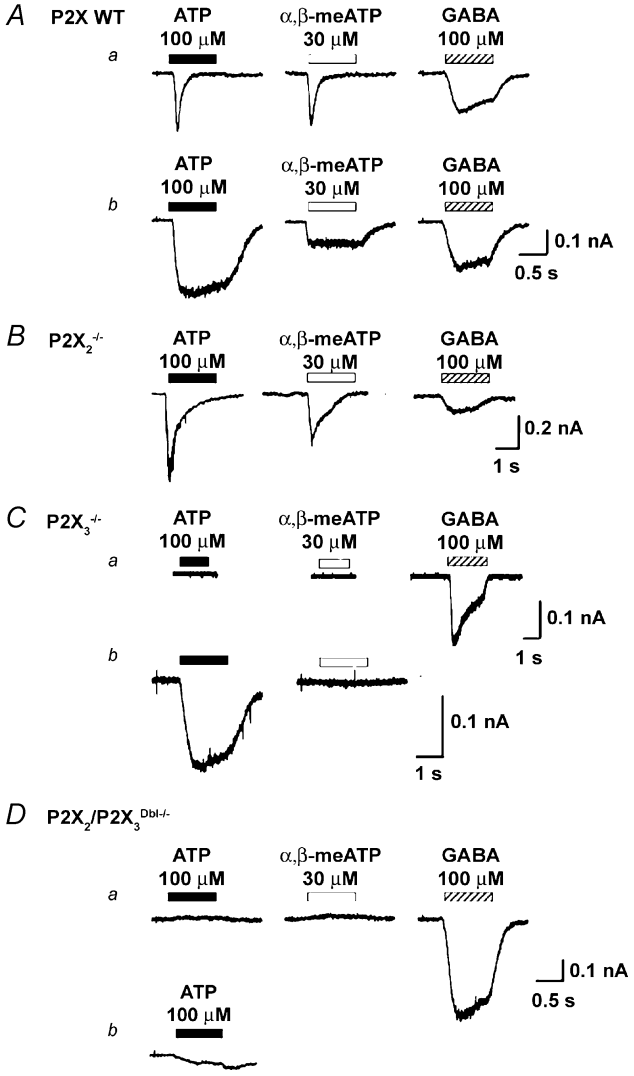

Figure 3. Whole-cell patch-clamp recordings of DRG neurones from $P2X_2^{-/-}$, $P2X_3^{-/-}$ and $P2X_2/P2X_3^{Dbl-/-}$ mice in response to P2X agonists
A, wild-type dorsal root ganglia (DRG) neurones (representative traces from $P2X_2/P2X_3^{Dbl+/+}$ mice) responded to ATP and α,β-meATP with either rapidly desensitizing (*a*) or sustained (*b*) responses; a composite response having both rapidly and slowly desensitizing components was also observed in some neurones (data not shown). All DRG neurones examined responded to 100 μM GABA with a sustained inward current. Comparable responses were seen in DRG neurones from all wild-type lines. *B*, in $P2X_2^{-/-}$ mice, DRG neurones all responded to ATP and α,β-meATP with rapidly desensitizing transient responses. *C*, in $P2X_3^{-/-}$ mice, many DRG neurones failed to respond to either ATP or α,β-meATP, but did respond to 100 μM GABA (*a*). Other $P2X_3^{-/-}$ neurones responded to ATP with a sustained inward current, but failed to respond to α,β-meATP (*b*). *D*, in $P2X_2/P2X_3^{Dbl-/-}$ mice, most DRG neurones failed to respond to ATP or α,β-meATP, but did respond to 100 μM GABA (*a*). A small percentage of neurones in double knockout mice gave small, very low amplitude responses to ATP (*b*), but did not respond to α,β-meATP (data not shown).

Table 2. Representative whole-cell patch-clamp data on peripheral ganglion neurons of $P2X_2$, $P2X_3$, and $P2X_2/P2X_{3Dbl}$ wild-type and knockout mice in response to 100 μM ATP

	WT		KO	
	Fraction of cells responding	Normalized response (pA/pF)	Fraction of cells responding	Normalized response (pA/pF)
$P2X_3$ KO[a]				
Nodose ganglion	44/46	202.7 ± 24.5	26/26	127.5 ± 33.2
DRG transient	26/61	10.8 ± 2.3	0/49[c]	NR[b]
DRG sustained	13/61	20.2 ± 8.5	6/49	4.3 ± 1.8
$P2X_2$ KO				
Nodose ganglion	9/9	180.2 ± 70.0	15/17	23.2 ± 6.1[e]
DRG transient	12/21	8.3 ± 0.8	17/24	14.0 ± 1.9
DRG sustained	5/21	45.2 ± 12.7	5/24	1.9 ± 0.8[f]
SCG	29/47	16.1 ± 8.1	1/35[c]	0.14
Coeliac ganglion	13/15	13.7 ± 4.2	0/14[c]	NR[b]
$P2X_2/P2X_3$ Dbl KO				
Nodose ganglion	21/21	138.5 ± 22.3	7/27[c]	0.5 ± 0.2[d]
DRG transient	7/18	38.6 ± 26.5	0/19[c]	NR[b]
DRG sustained	3/18	23.4 ± 17.9	7/19	0.9 ± 0.3
SCG	17/17	7.8 ± 2.8	4/11[c]	0.2 ± 0.04[e]

SCG, superior cervical ganglion; DRG, dorsal root ganglion. Data represent means ± S.E.M. of current amplitude normalized for membrane capacitance (pA/pF). [a]Patch-clamp data for $P2X_3^{-/-}$ mice were partly taken from Cockayne *et al.* (2000). [b]NR, nonresponder. A detection threshold of 0.01 nA was used to classify cells as responders or nonresponders. [c]$P < 0.005$, χ^2 test; [d]$P < 0.001$, [e]$P < 0.01$, [f]$P < 0.02$, unpaired *t* test.

per cystometrogram was decreased (8.9 ± 3.2 compared with 23.2 ± 4.4 for $P2X_2^{+/+}$ mice, $P < 0.05$) (Fig. 7*C*). To directly compare urodynamic function in mice lacking $P2X_2$ and/or $P2X_3$ receptor subunits, micturition contractions were similarly measured in $P2X_3^{-/-}$ and in $P2X_2/P2X_3^{Dbl-/-}$ mice. Consistent with previous findings (Cockayne *et al.* 2000), an increased threshold for micturition contractions was observed for $P2X_3^{-/-}$ mice (0.35 ± 0.09 ml compared with 0.12 ± 0.03 ml for $P2X_3^{+/+}$ mice, $P < 0.05$), while trends were observed for $P2X_2/P2X_3^{Dbl-/-}$ mice (0.22 ± 0.05 ml compared with 0.14 ± 0.04 ml for $P2X_2/P2X_3^{Dbl+/+}$ mice, $P = 0.164$). A trend to decreases in the average number of contractions per cystometrogram was observed for $P2X_3^{-/-}$ mice (20.0 ± 7.0 compared with 41.4 ± 10.7 for $P2X_3^{+/+}$ mice, $P = 0.136$) and $P2X_2/P2X_3^{Dbl-/-}$ mice (11.7 ± 5.8 compared with 32.7 ± 8.7 for $P2X_2/P2X_3^{Dbl+/+}$ mice, $P = 0.053$).

In vitro smooth muscle contractility of the urinary bladder in $P2X_3^{-/-}$, $P2X_2^{-/-}$ and $P2X_2/P2X_3^{Dbl-/-}$ mice

To ensure that the differences in urinary bladder reflex contractions observed in P2X-deficient mice (Fig. 7) were not caused by changes in the properties of the detrusor smooth muscle, we measured *in vitro* smooth muscle contractile responses of the urinary bladder. EFS of the urinary bladder induced parasympathetic nerve-mediated responses that were frequency dependent (Fig. 8*A–D*, control response) and abolished by 1 μM TTX (data not shown) in $P2X_2$, $P2X_3$ and $P2X_2/P2X_3$ wild-type and mutant mice (Fig. 8, and data not shown). Figure 8 illustrates representative data from $P2X_2/P2X_3^{Dbl+/+}$ (Fig. 8*A*, male; *C*, female) and $P2X_2/P2X_3^{Dbl-/-}$ (Fig. 8*B*, male; *D*, female) mice, where loss of $P2X_2$ and $P2X_3$ subunits had no effect on bladder smooth muscle responses to nerve-mediated stimulation (control responses). PPADS (30 μM) caused a significant inhibition of the response to EFS stimulation in all P2X wild-type and P2X-deficient mice (Fig. 8, and data not shown, $P < 0.001$). Interestingly, the PPADS-sensitive component was greater for female compared with male mice, and this was consistent for all groups of wild-type and null mutant mice (Fig. 8, and data not shown). The subsequent addition of atropine (1 μM) caused a further, almost complete, inhibition of responses in each group (Fig. 8 and data not shown, $P < 0.001$). Similarly, in the presence of atropine alone (1 μM, data not shown), there was significant inhibition of nerve-mediated responses for each group of mice, both male and female, and residual responses were almost completely inhibited

by the further addition of PPADS (30 μM, data not shown). No significant differences were observed in the inhibition by PPADS (30 μM) or atropine (1 μM) between the P2X wild-type and P2X-deficient mice of either sex.

We also measured detrusor smooth muscle contraction in response to a variety of agonists in $P2X_2^{-/-}$, $P2X_3^{-/-}$ and $P2X_2/P2X_3^{Dbl-/-}$ mice. Carbachol (0.01–300 μM) caused concentration-dependent contractions of the detrusor smooth muscle, and no differences were seen in the concentration response curves, or in calculated pD_2 values ($-\log EC_{50}$ concentration) between male or female P2X wild-type and P2X-deficient mice (data not shown). Both ATP (0.1 μM–1 mM) and β,γ-meATP (0.1–300 μM) caused transient concentration-dependent contractions of the detrusor smooth muscle, and no differences were seen in the concentration–response curves for either of these agonists between male or female, wild-type and null mutant mice (data not shown). As neither agonist reached a maximum response, pD2 values could not be calculated. Lastly, substance P (0.3 μM), 5-HT (100 μM), and histamine (100 μM) each caused contraction of the detrusor smooth muscle, and no differences were seen between male or female P2X wild-type and P2X-deficient mice (data not shown).

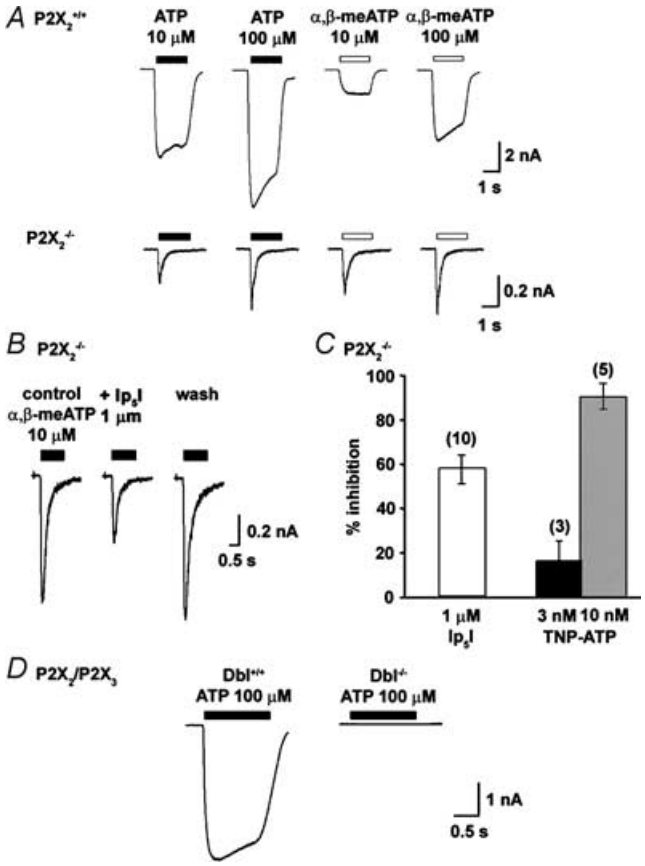

Figure 4. Whole-cell patch-clamp recordings of nodose ganglion neurones from $P2X_2^{-/-}$ and $P2X_2/P2X_3^{Dbl-/-}$ mice in response to P2X agonists

A, comparison of responses to ATP and α,β-meATP recorded from nodose ganglion neurones of $P2X_2^{+/+}$ and $P2X_2^{-/-}$ mice. Wild-type neurones gave a sustained inward current to both agonists, while neurones from $P2X_2^{-/-}$ mice responded with a rapidly desensitizing transient response. *B* and *C*, antagonist sensitivity of the remaining α,β-meATP response recorded in $P2X_2^{-/-}$ nodose neurones. *B*, representative responses to 10 μM α,β-meATP recorded from a single nodose neurone before, in the presence of, and after washing out the antagonist 1 μM diinosine pentaphosphate (Ip_5I).
C, histogram comparing the antagonist effect of 1 μM Ip_5I with that of 3 nM and 10 nM TNP-ATP. Data represent means ± S.E.M. from the number of neurones shown in parenthesis. *D*, comparison of responses to ATP recorded in nodose ganglion neurones from $P2X_2/P2X_3^{Dbl+/+}$ and $P2X_2/P2X_3^{Dbl-/-}$ mice.

Activity of pelvic afferent fibres evoked by distension of the bladders of $P2X_3^{-/-}$, $P2X_2^{-/-}$ and $P2X_2/P2X_3^{Dbl-/-}$ mice

To further investigate the sensory role of P2X receptor subtypes within the urinary bladder, we measured the sensitivity of bladder afferents to distension in P2X-deficient mice in a urinary bladder/pelvic nerve preparation (Vlaskovska *et al.* 2001). The representative traces shown in Fig. 9 illustrate the delayed afferent responsiveness to bladder distension in $P2X_3^{-/-}$, $P2X_2^{-/-}$, and $P2X_2/P2X_3^{Dbl-/-}$ mice, compared to P2X wild-type controls. Volume and pressure thresholds for afferent activation were calculated as shown in the top panel of Fig. 10. The volume thresholds for whole-nerve activation were significantly elevated in $P2X_2^{-/-}$

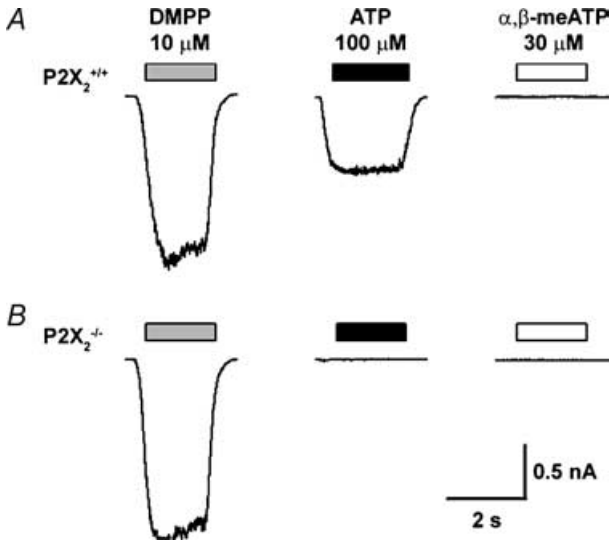

Figure 5. Whole-cell patch-clamp recordings of SCG neurones from $P2X_2^{-/-}$ mice in response to ATP

A, SCG neurones from $P2X_2^{+/+}$ mice gave a robust sustained inward current to ATP and the nicotinic agonist DMPP, but not to α,β-meATP. *B*, SCG neurones from $P2X_2^{-/-}$ mice responded to DMPP, but there was no response to ATP or α,β-meATP.

mice (0.32 ± 0.05 ml compared with 0.17 ± 0.03 ml for $P2X_2^{+/+}$ mice, $P < 0.05$). Similarly, the volume thresholds were increased in $P2X_3^{-/-}$ mice (0.38 ± 0.06 ml compared with 0.14 ± 0.02 ml for $P2X_3^{+/+}$ mice, $P < 0.01$), and $P2X_2/P2X_3^{Dbl-/-}$ mice (0.38 ± 0.06 ml compared with 0.13 ± 0.03 ml for $P2X_2/P2X_3^{Dbl+/+}$ mice, $P < 0.01$) (Fig. 10*A*). The pressure thresholds of bladder afferents in P2X-deficient mice also appeared to be elevated, but the differences were not significant ($P > 0.05$) (Fig. 10*B*).

We further investigated the pressure–response relationships of whole nerves and single units in P2X wild-type and P2X-deficient mice by comparing the mean levels of activity at various intraluminal pressures. At each pressure level, the mean values of whole-nerve discharge rate were lower in all P2X-deficient mice compared with P2X wild-type controls, although the difference was not statistically significant (Fig. 10*C*). However, the mean values of single unit discharge rate at pressures between 20 and 50 mmHg were significantly lower in P2X-deficient mice compared with wild-type controls (Fig. 10*D*). The pressure–response relationships could be fitted with a Boltzmann sigmoidal equation, and the curves for all P2X-deficient mice had shallower slopes compared with those for P2X wild-type controls.

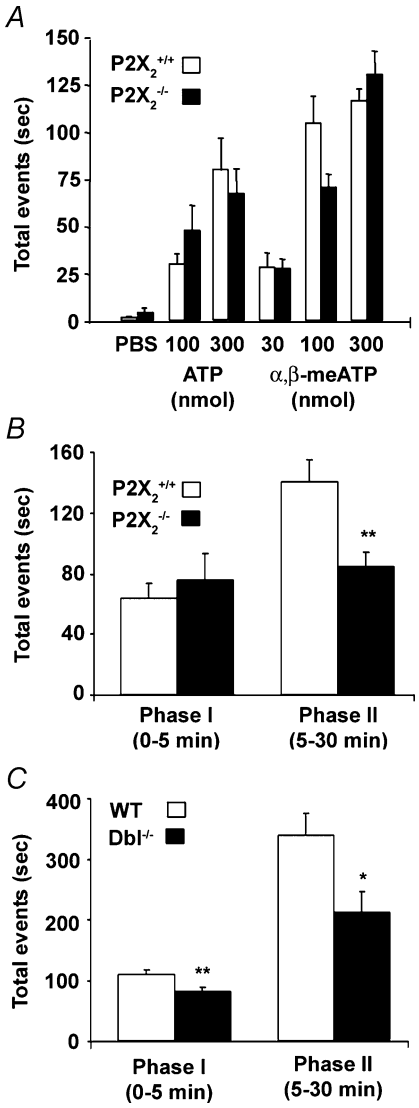

Figure 6. P2X agonist and formalin-evoked nociceptive responses in $P2X_2^{-/-}$ and $P2X_2/P2X_3^{Dbl-/-}$ mice
A, hindpaw lifting response in 2- to 3-month-old female $P2X_2^{+/+}$ (open bars) and $P2X_2^{-/-}$ (filled bars) mice ($n = 8$–10) following intraplantar injection of varying doses of ATP or α,β-meATP in a total volume of 30 μl. Data represent the means ± S.E.M. of the total time spent lifting the treated paw in a 4 min time bin following administration of compound. *B* and *C*, nociceptive behavioural response in 3-month-old male and female $P2X_2^{+/+}$ (*B*, open bars) and $P2X_2^{-/-}$ (*B*, filled bars) mice ($n = 9$–11), or 3- to 4-month-old male $P2X_2/P2X_3^{Dbl+/+}$ (*C*, open bars) and $P2X_2/P2X_3^{Dbl-/-}$ (*C*, filled bars) mice ($n = 12$) following intraplantar injection of 5% formalin in a total volume of 20 μl. Data represent the means ± S.E.M. of the total time spent licking, biting or flinching the treated paw in the 0–5 and 5–30 min time bins following administration of formalin. $^*P < 0.05$, $^{**}P < 0.01$; Wilcoxon rank-sum exact test.

Discussion

The present study supports several important conclusions about the role of $P2X_2$ and $P2X_3$ subunits in mediating certain sensory functions of ATP. First, electrophysiological studies indicate that $P2X_2$ and $P2X_3$ subunits account for virtually all ATP-mediated responses in mouse sensory and sympathetic ganglion neurones. Second, our data support a role for $P2X_2$ subunits in mediating pain-related behaviour. Lastly, the consistent finding of bladder hyporeflexia and reduced activity of pelvic afferent fibres in response to bladder filling, in mice lacking $P2X_2$ and/or $P2X_3$ receptor subunits, supports the involvement of both $P2X_3$ and $P2X_{2/3}$ receptors in mediating mechanosensory transduction within the urinary bladder.

Electrophysiological studies in P2X-deficient mice have helped to define the contribution of $P2X_2$, $P2X_3$ and $P2X_{2/3}$ receptors to ATP responses on sensory and autonomic ganglion neurones. In DRG sensory neurones, ATP and α,β-meATP induce rapidly desensitizing, slowly desensitizing or biphasic currents, consistent with $P2X_3$ and $P2X_{2/3}$ receptors (Rae *et al.* 1998; Burgard *et al.* 1999). Previous studies in $P2X_3^{-/-}$ mice confirmed these observations (Cockayne *et al.* 2000; Zhong *et al.* 2001), with ∼90% of DRG neurones having no response to ATP or α,β-meATP, and only a small percentage (∼12%) responding only to ATP with slowly desensitizing currents. In contrast, nodose ganglion neurones contain predominantly $P2X_2$ and $P2X_{2/3}$ receptors (Virginio *et al.* 1998; Thomas *et al.* 1998), with virtually all ATP and α,β-meATP responses being slowly desensitizing. In $P2X_3^{-/-}$ mice slowly desensitizing responses to α,β-meATP were lost, while sustained responses to ATP were maintained (Cockayne *et al.* 2000; Zhong *et al.* 2001). Taken together, these data supported the idea that

ATP-induced currents in DRG neurones are mediated largely by $P2X_3$ receptors, while in nodose neurones $P2X_2$ and $P2X_{2/3}$ receptors appear more important. In the present study, we extended these findings with whole-cell patch-clamp recordings from $P2X_2^{-/-}$ and $P2X_2/P2X_3^{Dbl-/-}$ mice. Removal of the $P2X_2$ subunit left only a rapidly desensitizing response in both DRG and nodose ganglion neurones in response to ATP or α,β-meATP, consistent with the loss of slowly desensitizing $P2X_2$ and $P2X_{2/3}$ receptors. The antagonist sensitivity of the remaining α,β-meATP response in nodose neurones was consistent with a $P2X_3$ receptor: greater than 50% inhibition by 1 μM Ip_5I, and almost complete inhibition by 10 nM TNP-ATP. Finally, in $P2X_2/P2X_3^{Dbl-/-}$ mice virtually all ATP currents were lost in DRG and nodose ganglion neurones, supporting the view that $P2X_2$ and $P2X_3$ subunits are the predominant functional P2X receptors expressed in mouse sensory neurones. Sensory ganglia in $P2X_2/P2X_3^{Dbl-/-}$ mice were of normal size and histological appearance, with no apparent loss of neurones. The presence of a small residual sustained response to ATP in some DRG and nodose neurones from $P2X_2/P2X_3^{Dbl-/-}$ mice indicates the presence of low levels of other P2X subunits or P2Y receptors in some neurones. $P2Y_1$ and $P2Y_2$ could play a minor role as these receptors are ATP-sensitive, and have been colocalized on sensory neurones with $P2X_3$ and TRPV1 receptors (Ruan & Burnstock, 2003; Gerevich & Illes, 2005). Because of the low amplitude of these responses, we have not investigated them further.

Our findings from sympathetic ganglion neurones indicate a predominant functional role for $P2X_2$-containing receptors (probably $P2X_2$ homomultimers). Thus, absence of the $P2X_2$ subunit leads to an almost complete loss of ATP responses in coeliac and SCG neurones. These data are consistent with the known pharmacology of P2X receptors in cultured autonomic ganglion neurones (Khakh *et al.* 1995; Zhong *et al.*

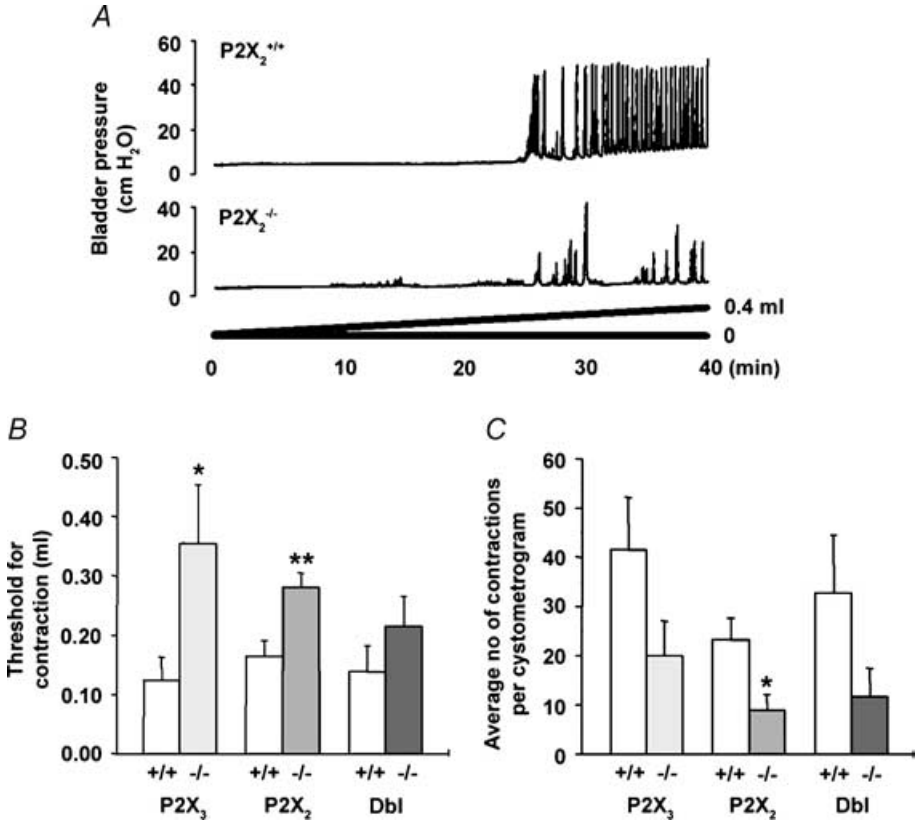

Figure 7. Urinary bladder cystometry in $P2X_3^{-/-}$, $P2X_2^{-/-}$ and $P2X_2/P2X_3^{Dbl-/-}$ mice
A, representative acute cystometrograms recorded from anaesthetized and transurethrally catheterized 5- to 6-month-old female $P2X_2^{+/+}$ and $P2X_2^{-/-}$ mice. Traces illustrate bladder pressure recorded in response to a constant intravesical infusion of saline (10 μl min^{-1} for 40 min). Contractions greater than 20 cm H_2O were taken as micturition contractions. *B* and *C*, quantification of the threshold for contraction (*B*) and the average number of contractions per cystometrogram (*C*) for 5- to 6-month-old female $P2X_3^{-/-}$ ($n = 7$), $P2X_2^{-/-}$ ($n = 10$) and $P2X_2/P2X_3^{Dbl-/-}$ ($n = 7$) mice tested in parallel, under similar conditions, with their respective wild-type controls ($P2X_3^{+/+}$ and $P2X_2/P2X_3^{Dbl+/+}$ $n = 7$, $P2X_2^{+/+}$ $n = 11$). Data represent the means ± S.E.M. $^*P < 0.05$, $^{**}P < 0.01$; Wilcoxon rank-sum exact test.

2000). As with sensory neurones, the presence of small ATP responses in a few sympathetic neurones suggests the presence of low levels of some other P2 receptors. Whether this expression is normally present or the result of compensatory upregulation is unclear. Studies using $P2X_1$-deficient mice have suggested that $P2X_1$ receptor subunits can contribute to heteromultimeric $P2X_2$ receptors in a small population of mouse SCG neurones (Calvert, 2004).

$P2X_3$ and $P2X_{2/3}$ receptors are gaining recognition for their importance in facilitating pain transmission (Jarvis, 2003), but the differential contribution of these receptors to specific pain-related behaviours is still poorly understood. An assessment of pain-related behaviours in $P2X_2^{-/-}$ mice revealed deficits in nocifensive responses in the persistent, but not acute phase of the formalin model, no alterations in acute nocifensive responses to intraplantar injection of P2X agonists, and no attenuation of acute thermal nociceptive responses in the tail flick or plantar test. These data suggest that $P2X_{2/3}$ (and $P2X_2$) receptors are probably not critical to acute nociceptive responses. These data also suggest that homomultimeric $P2X_3$ receptors are sufficient to account for $P2X_3$-dependent nocifensive responses to ATP or α,β-meATP. This is consistent with the observed deficits in P2X agonist-induced nocifensive responses in $P2X_3^{-/-}$ mice (Cockayne *et al.* 2000), and in rats following intraplantar administration of A-317491 (McGaraughty *et al.* 2003). Inoue *et al.* (2003) have also shown that $P2X_3$ antisense inhibits multiple pain-related behaviours induced by intraplantar α,β-meATP, including nocifensive behaviour, thermal hyperalgesia and mechanical allodynia, while only the latter is inhibited by $P2X_2$ antisense. In addition to $P2X_3$ receptors, it is reasonable to speculate that additional P2X or P2Y receptors are involved in the pain-producing effects of ATP. Accordingly, the reduction in nocifensive lifting in $P2X_3^{-/-}$ mice was suppressed by only ~50%, but a further reduction in the residual response was produced by the non-selective P2 receptor antagonist PPADS (Cockayne *et al.* 2000).

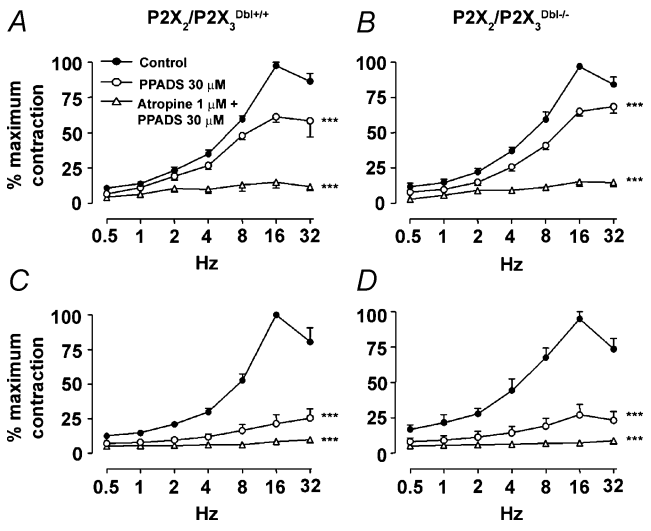

Figure 8. Frequency–response curves of the purinergic and cholinergic components of nerve-mediated responses in bladders of $P2X_2/P2X_3^{Dbl-/-}$ mice

Representative frequency–response curves in the absence (control) and presence of PPADS (30 μM), and finally in the presence of both PPADS (30 μM) and atropine (1 μM) for (*A*) male $P2X_2/P2X_3^{Dbl+/+}$ mice ($n = 5$), (*B*) male $P2X_2/P2X_3^{Dbl-/-}$ mice ($n = 6$), (*C*) female $P2X_2/P2X_3^{Dbl+/+}$ mice ($n = 5$), and (*D*) female $P2X_2/P2X_3^{Dbl-/-}$ mice ($n = 5$). Electrical field stimulation (EFS) was carried out at 100 V, 0.3 ms, 0.5–32 Hz, with 15 s stimulation. Data represent the means ± S.E.M. of the percentage of the maximum control response. ***$P < 0.001$; two-way analysis of variance (ANOVA).

In the formalin model, deficits in only the persistent phase in $P2X_2^{-/-}$ mice contrasts with findings from $P2X_3^{-/-}$ mice (Cockayne *et al.* 2000; Souslova *et al.* 2000), or from rats following intradermal administration of TNP-ATP or A-317491 (Jarvis *et al.* 2001; McGaraughty *et al.* 2003), where attenuated responses were seen in both acute and persistent formalin-induced nociception. These data suggest that $P2X_{2/3}$ (and $P2X_2$) receptors are not critical to the acute nociceptive effects of formalin, but are a necessary component of the second phase of the formalin response, where they may contribute to the underlying changes in central sensitization believed to be associated with persistent inflammatory pain. These findings are consistent with the idea that presynaptic $P2X_3$ and/or $P2X_{2/3}$ receptors may be important in ATP-mediated facilitation of glutamate release from primary sensory afferents in the dorsal horn of the spinal cord (Gu & MacDermott, 1997; Nakatsuka & Gu, 2001; Nakatsuka *et al.* 2003). Whether homomeric $P2X_2$ receptors, or heteromeric receptors containing the $P2X_2$ subunit (other than $P2X_{2/3}$), also contribute to persistent pain responses is not entirely clear; however, it has been suggested that pre- and postsynaptic $P2X_2$ receptors may be involved in some aspects spinal nociceptive processing (Bardoni *et al.* 1997; Hugel & Schlichter, 2000). It will be intriguing to determine whether the mechanism(s) underlying the potentially distinct but overlapping roles for $P2X_3$ and $P2X_{2/3}$ receptors reflects differential regulation of receptor function within single neurones, or rather reflects differential expression patterns within neurones playing distinct coding roles. Nevertheless, our data are consistent with recent findings (Jarvis, 2003) that $P2X_3$ receptors mediate some aspects of acute nociception, while $P2X_{2/3}$ receptors appear to play a more prominent role in persistent inflammatory pain and some aspects of central sensitization (e.g. neuropathic pain). Deficits in both the acute and persistent phase of the formalin response in $P2X_2/P2X_3^{Dbl-/-}$ mice are consistent with this interpretation. Studies with mice lacking $P2X_2$ and/or $P2X_3$ receptor subunits in additional models of chronic

inflammatory and neuropathic pain may help elucidate this further.

$P2X_3$-containing receptors also play an important role in visceral mechanosensory transduction. Within the urinary bladder, it is proposed that ATP released from the uroepithelium signals the extent of distension and activates $P2X_3$ receptors on adjacent primary afferent nerve fibres; thus conveying information on bladder 'fullness' to spinal and supraspinal centres coordinating the micturition reflex. Previously, we demonstrated that $P2X_3^{-/-}$ mice had reduced urinary bladder reflexes (Cockayne *et al.* 2000), and a delayed threshold for activation of pelvic nerve afferents in response to distension (Vlaskovska *et al.* 2001). In the present study, a direct comparison of cystometric function across $P2X_2^{-/-}$, $P2X_3^{-/-}$ and $P2X_2/P2X_3^{Dbl-/-}$ mice showed a consistent finding of urinary bladder hyporeflexia. Myographic responses of isolated bladders were normal in these mice, as no changes were observed in responsiveness to neurogenic stimulation, or to stimulation with a variety of neurotransmitters acting via muscarinic, purinergic, histamine, or neurokinin receptors. These findings support the conclusion that bladder hyporeflexia in P2X-deficient mice results from changes in sensory and not motor function. Supporting these sensory findings, bladder afferents from P2X-deficient mice had altered electrophysiological responses, as measured by an increased threshold for activation of pelvic nerve afferents in response to bladder distension. These data extend our previous findings from $P2X_3^{-/-}$ mice, and indicate that $P2X_3$ and $P2X_{2/3}$ receptors on bladder afferent terminals are important in mechanosensory transduction within the urinary bladder. These findings are consistent with those of Zhong *et al.* (2003) that bladder sensory neurones projecting via the pelvic nerve express predominantly $P2X_{2/3}$ receptors (Zhong *et al.* 2003). In this study, whole-cell patch-clamp recordings of labelled bladder pelvic afferents revealed that ~90% of bladder afferent neurones responded to ATP and α,β-meATP with persistent, TNP-ATP-sensitive currents. In the present study, single-unit activity measurements

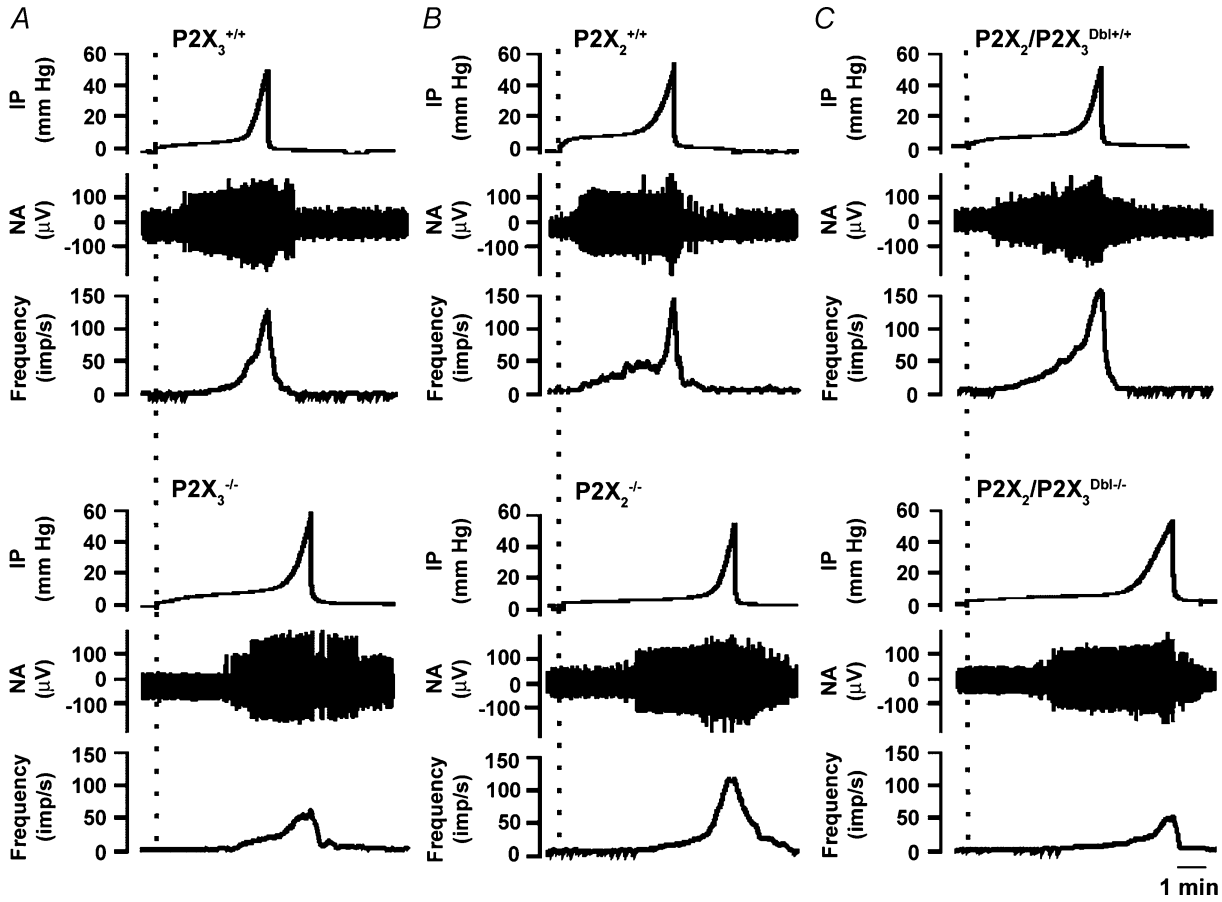

Figure 9. Pelvic nerve response to bladder filling in $P2X_3^{-/-}$, $P2X_2^{-/-}$ and $P2X_2/P2X_3^{Dbl-/-}$ mice
Representative traces of intraluminal pressure (IP), whole-nerve activity (NA), and whole-nerve discharge rate (frequency) are shown for $P2X_3$ (left), $P2X_2$ (middle) and $P2X_2/P2X_3^{Dbl}$ (right) wild-type (upper panels) and mutant (lower panels) mice. The dotted lines indicate the start of bladder distension at a constant rate of 0.1 ml min^{-1}. Note the marked delay in bladder afferent activation in P2X-deficient mice.

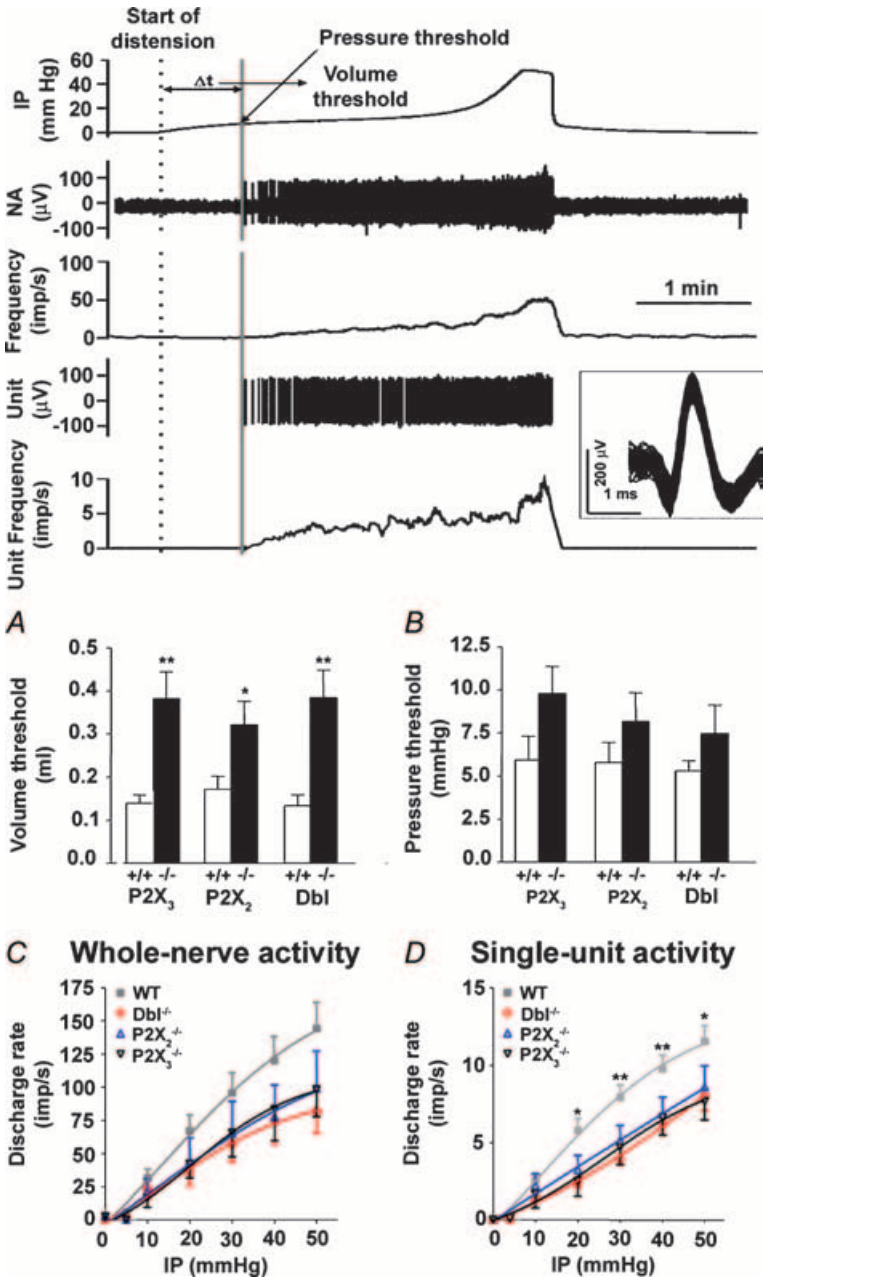

Figure 10. Threshold for whole-nerve response to bladder distension and single unit discrimination reveals a reduced sensitivity of pelvic afferents in P2X-deficient mice

Top panel, the upper three traces are intraluminal pressure (IP), whole-nerve activity (NA) and whole-nerve discharge rate (frequency). The lower two traces are a single-unit spike (Unit) and its discharge rate (unit frequency). In the inset are superimposed spikes of that unit showing little variation in waveform. The dotted line indicates the start of bladder filling and the second solid line indicates the start of nerve firing (pressure threshold). Volume threshold is calculated from the interval between those two lines and the rate of bladder filling (0.1 ml min^{-1}). Bottom panel, reduced sensitivity of pelvic afferents to bladder filling in $P2X_3^{-/-}$, $P2X_2^{-/-}$ and $P2X_2/P2X_3^{Dbl-/-}$ mice. *A*, volume thresholds were significantly increased in P2X-deficient mice ($n = 7$–10) compared with the respective wild-type controls ($n = 6$–12). *B*, pressure thresholds were not significantly different between P2X-deficient mice ($n = 6$–10) and wild-type controls ($n = 6$–9). *C*, the pressure–response curves of whole nerves (*C*) and single units (*D*) in P2X-deficient mice showed shallower slopes compared with wild-type mice. $^*P < 0.05$ and $^{**}P < 0.01$ comparing the mean discharge frequency of wild-type mice with P2X-deficient mice at various intraluminal pressure levels; two way analysis of variance (ANOVA).

also confirmed that afferent mechanosensitivity was reduced in P2X-deficient mice. However, additional experimentation will be needed to investigate whether P2X deletions confer changes in the sensitivity of low threshold Aδ, or high threshold C-fibre afferents. Studies in cat have shown that Aδ afferents respond in a graded manner to bladder distension, but can also be activated by noxious stimuli (Janig & Morrison, 1986), while C fibres have high mechanical thresholds and are sensitized by inflammatory mediators (Habler *et al.* 1990). ATP and α,β-meATP not only activate both low- and high-threshold bladder afferents directly, but also sensitize their mechanosensory responses (Vlaskovska *et al.* 2001; Rong *et al.* 2002). Thus, $P2X_3$ and $P2X_{2/3}$ receptors may be important in sensing volume changes during normal bladder filling, but may also participate in lowering the threshold for afferent activation in pathological circumstances.

In summary, we have demonstrated that $P2X_2$ and $P2X_3$ subunits account for virtually all ATP responses in sensory and autonomic ganglion neurones. We have also shown that in addition to $P2X_3$ receptors, $P2X_{2/3}$ receptors (and possibly $P2X_2$) are important in sensory modulation in at least one model of persistent pain and in the regulation of urinary bladder reflexes. While gene deletion in mice can result in compensatory changes *in vivo* that may contribute to observed behavioural phenotypes, our collective data on pain-related behaviours in $P2X_2^{-/-}$, $P2X_3^{-/-}$ and $P2X_2/P2X_3^{Dbl-/-}$ mice are consistent with data generated using the dual $P2X_3$, $P2X_{2/3}$ receptor antagonist A-317491 (Jarvis *et al.* 2002; McGaraughty *et al.* 2003; Wu *et al.* 2004), $P2X_3$ deletion (Souslova *et al.* 2000), or antisense (Honore *et al.* 2002*a*; Barclay *et al.* 2002; Inoue *et al.* 2003) and siRNA (Dorn *et al.* 2004) knock-down approaches of $P2X_3$ or $P2X_2$ receptor expression. Taken together, these data support an important role for *both* $P2X_3$ and $P2X_{2/3}$ receptors in mediating potentially distinct, but overlapping, roles in pain transmission. Given the interest in investigating selective $P2X_3$ and $P2X_{2/3}$ antagonists for conditions of inflammatory or neuropathic pain, and disorders of urine storage and voiding, such as overactive bladder, it will be essential to understand the differential role of these receptors in somatic and visceral mechanosensory pathways, as well as the relative importance of peripheral and central $P2X_3$-containing receptors. However, evidence to date suggests that antagonism of $P2X_3$ and $P2X_{2/3}$ receptors s may have therapeutic potential in the treatment of these conditions.

References

Barclay J, Patel S, Dorn G, Wotherspoon G, Moffatt S & Eunson L *et al.* (2002). Functional downregulation of $P2X_3$ receptor subunit in rat sensory neurons reveals a significant role in chronic neuropathic and inflammatory pain. *J Neurosci* **22**, 8139–8147.

Bardoni R, Goldstein PA, Lee CJ, Gu JG & MacDermott AB (1997). ATP P2X receptors mediate fast synaptic transmission in the dorsal horn of the rat spinal cord. *J Neurosci* **17**, 5297–5304.

Bertrand PP & Bornstein JC (2002). ATP as a putative sensory mediator: activation of intrinsic sensory neurons of the myenteric plexus via P2X receptors. *J Neurosci* **22**, 4767–4775.

Bian X, Ren J, DeVries M, Schnegelsberg B, Cockayne DA, Ford APDW & Galligan JJ (2003). Peristalsis is impaired in the small intestine of mice lacking the $P2X_3$ subunit. *J Physiol* **551**, 309–322.

Bland-Ward PA & Humphrey PPA (1997). Acute nociception mediated by hindpaw P2X receptor activation in the rat. *Br J Pharmacol* **122**, 365–371.

Burgard EC, Niforatos W, Van Biesen T, Lynch KJ, Touma E, Metzger RE, Kowaluk EA & Jarvis MF (1999). P2X receptor-mediated ionic currents in dorsal root ganglion neurons. *J Neurophysiol* **82**, 1590–1598.

Burnstock G (2000). P2X receptors in sensory neurons. *Br J Anaesth* **84**, 476–488.

Burnstock G (2001). Purine-mediated signalling in pain and visceral perception. *Trends Pharmacol Sci* **22**, 182–188.

Burnstock G (2003). Purinergic receptors in the nervous system. In *Current Topics in Membranes*, vol. 54, ed. Schwiebert EM, pp. 307–368. Academic Press, San Diego.

Calvert JA (2004). Heterogeneity of P2X receptors in sympathetic neurons: contribution of neuronal $P2X_1$ receptors revealed using knockout mice. *Mol Pharmacol* **65**, 139–148.

Cockayne DA, Hamilton SG, Zhu Q-M, Dunn PM, Zhong Y, Novakovic S *et al.* (2000). Urinary bladder hyporeflexia and reduced pain-related behavior in $P2X_3$-deficient mice. *Nature* **407**, 1011–1015.

Dmitrieva N, Shelton D, Rice AS & McMahon SB (1997). The role of nerve growth factor in a model of visceral inflammation. *Neuroscience* **78**, 449–459.

Dorn G, Patel S, Wotherspoon G, Hemmings-Mieszczak M, Barclay J, Natt FJC, Martin P, Bevan S, Fox A, Ganju P, Wishart W & Hall J (2004). siRNA relieves chronic neuropathic pain. *Nucleic Acids Res* **32**, e49.

Dunn PM, Benton DC, Campos Rosa J, Ganellin CR & Jenkinson DH (1996). Discrimination between subtypes of apamin-sensitive Ca^{2+}-activated K^+ channels by gallamine and a novel bis-quaternary quinolinium cyclophane, UCL 1530. *Br J Pharmacol* **117**, 35–42.

Dunn PM, Zhong Y & Burnstock G (2001). P2X receptors in peripheral neurons. *Prog Neurobiol* **65**, 107–134.

Ferguson DR, Kennedy I & Burton TJ (1997). ATP is released from rabbit urinary bladder epithelial cells by hydrostatic pressure changes – a possible sensory mechanism? *J Physiol* **505**, 503–511.

Gerevich Z & Illes P (2005). P2Y receptors and pain transmission. *Purinergic Signal* **1**, 3–10.

Gu JG & MacDermott AB (1997). Activation of ATP P2X receptors elicits glutamate release from sensory neuron synapses. *Nature* **389**, 749–753.

Habler HJ, Janig W & Koltzenburg M (1990). Activation of unmyelinated afferent fibres by mechanical stimuli and inflammation of the urinary bladder in the cat. *J Physiol* **425**, 545–562.

Honore P, Kage K, Mikusa J, Watt AT, Johnston JF, Wyatt JR, Faltynek CR, Jarvis MF & Lynch K (2002*a*). Analgesic profile of intrathecal $P2X_3$ antisense oligonucleotide treatment in chronic inflammatory and neuropathic pain states in rats. *Pain* **99**, 11–19.

Honore P, Mikusa J, Bianchi B, McDonald H, Cartmell J, Faltynek C & Jarvis MF (2002*b*). TNP-ATP, a potent $P2X_3$ receptor antagonist, blocks acetic acid-induced abdominal constriction in mice: comparison with reference analgesics. *Pain* **96**, 99–105.

Hugel S & Schlichter R (2000). Presynaptic P2X receptors facilitate inhibitory GABAergic transmission between cultured rat spinal cord dorsal horn neurons. *J Neurosci* **20**, 2121–2130.

Inoue K, Tsuda M & Koizumi S (2003). ATP induced three types of pain behaviors, including allodynia. *Drug Dev Res* **59**, 56–63.

Janig W & Morrison JF (1986). Functional properties of spinal visceral afferents supplying abdominal and pelvic organs, with special emphasis on visceral nociception. *Prog Brain Res* **67**, 87–114.

Jarvis MF (2003). Contributions of $P2X_3$ homomeric and heteromeric channels to acute and chronic pain. *Expert Opin Ther Targets* **7**, 513–522.

Jarvis MF, Burgard EC, McGaraughty S, Honore P, Lynch K, Brennan TJ *et al.* (2002). A-317491, a novel potent and selective non-nucleotide antagonist of $P2X_3$ and $P2X_{2/3}$ receptors, reduces chronic inflammatory and neuropathic pain in the rat. *Proc Natl Acad Sci U S A* **99**, 17179–17184.

Jarvis MF, Wismer CT, Schweitzer E, Yu H, Van Biesen T, Lynch KJ, Burgard EC & Kowaluk EA (2001). Modulation of BzATP and formalin induced nociception: attenuation by the P2X receptor antagonist, TNP-ATP and enhancement by the $P2X_3$ allosteric modulator, cibacron blue. *Br J Pharmacol* **132**, 259–269.

Khakh BS, Humphrey PP & Surprenant A (1995). Electrophysiological properties of P2X-purinoceptors in rat superior cervical, nodose and guinea-pig coeliac neurones. *J Physiol* **484**, 385–395.

King BF, Liu M, Pintor J, Gualix J, Miras-Portugal MT & Burnstock G (1999). Diinosine pentaphosphate (IP_5I) is a potent antagonist at recombinant rat $P2X_1$ receptors. *Br J Pharmacol* **128**, 981–988.

Kirkup AJ, Booth CE, Chessell IP, Humphrey PPA & Grundy D (1999). Excitatory effect of P2X receptor activation on mesenteric afferent nerves in the anaesthetised rat. *J Physiol* **520**, 551–563.

Knight GE, Bodin P, De Groat WC & Burnstock G (2002). ATP is released from guinea pig ureter epithelium on distension. *Am J Physiol Renal Physiol* **282**, F281–288.

McGaraughty S, Wismer CT, Zhu CZ, Mikusa J, Honore P, Chu KL *et al.* (2003). Effects of A-317491, a novel and selective $P2X_3$/$P2X_{2/3}$ receptor antagonist, on neuropathic, inflammatory and chemogenic nociception following intrathecal and intraplantar administration. *Br J Pharmacol* **140**, 1381–1388.

Nakatsuka T & Gu JG (2001). ATP P2X receptor-mediated enhancement of glutamate release and evoked EPSCs in dorsal horn neurons of the rat spinal cord. *J Neurosci* **21**, 6522–6531.

Nakatsuka T, Tsuzuki K, Ling JX, Sonobe H & Gu JG (2003). Distinct roles of P2X receptors in modulating glutamate release at different primary sensory synapses in rat spinal cord. *J Neurophysiol* **89**, 3243–3252.

North RA (2002). Molecular physiology of P2X receptors. *Physiol Rev* **82**, 1013–1067.

Pandita RK & Andersson K-E (2004). Intravesical adenosine triphosphate stimulates the micturition reflex in awake, freely moving rats. *J Urol* **168**, 1230–1234.

Rae MG, Rowan EG & Kennedy C (1998). Pharmacological properties of $P2X_3$-receptors present in neurones of the rat dorsal root ganglia. *Br J Pharmacol* **124**, 176–180.

Rong W, Spyer KM & Burnstock G (2002). Activation and sensitisation of low and high threshold afferent fibres mediated by P2X receptors in the mouse urinary bladder. *J Physiol* **541**, 591–600.

Ruan HZ & Burnstock G (2003). Localisation of $P2Y_1$ and $P2Y_4$ receptors in dorsal root, nodose and trigeminal ganglia of the rat. *Histochem Cell Biol* **120**, 415–426.

Silva AJ, Simpson EM, Takahashi JS, Lipp HP, Nakanishi S, Wehner JM, Giese KP, Tully T, Abel T & Chapman PF (1997). Mutant mice and neuroscience: recommendations concerning genetic background. *Neuron* **19**, 755–759.

Souslova V, Cesare P, Ding Y, Akopian AN, Stanfa L, Suzuki R *et al.* (2000). Warm-coding deficits and aberrant inflammatory pain in mice lacking $P2X_3$ receptors. *Nature* **407**, 1015–1017.

Sun Y & Chai TC (2002). Effects of dimethyl sulphoxide and heparin on stretch-activated ATP release by bladder urothelial cells from patients with interstitial cystitis. *BJU Int* **90**, 381–385.

Thomas S, Virginio C, North RA & Surprenant A (1998). The antagonist trinitrophenyl-ATP reveals co-existence of distinct P2X receptor channels in rat nodose neurones. *J Physiol* **509**, 411–417.

Tsuda M, Koizumi S, Kita A, Shigemoto Y, Ueno S & Inoue K (2000). Mechanical allodynia caused by intraplantar injection of P2X receptor agonist in rats: involvement of heteromeric $P2X_{2/3}$ receptor signaling in capsaicin-insensitive primary afferent neurons. *J Neurosci* **20**, 90RC.

Tsuda M, Ueno S & Inoue K (1999*a*). Evidence for the involvement of spinal endogenous ATP and P2X receptors in nociceptive responses caused by formalin and capsaicin in mice. *Br J Pharmacol* **128**, 1497–1504.

Tsuda M, Ueno S & Inoue K (1999*b*). In vivo pathway of thermal hyperalgesia by intrathecal administration of α,β-methylene ATP in mouse spinal cord: Involvement of the glutamate-NMDA receptor system. *Br J Pharmacol* **127**, 449–456.

Ueno S, Moriyama T, Honda K, Kamiya H, Sakurada T & Katsuragi T (2003). Involvement of $P2X_2$ and $P2X_3$ receptors in neuropathic pain in a mouse model of chronic constriction injury. *Drug Dev Res* **59**, 104–111.

Virginio C, Robertson G, Surprenant A & North RA (1998). Trinitrophenyl-substituted nucleotides are potent antagonists selective for $P2X_1$, $P2X_3$, and heteromeric $P2X_{2/3}$ receptors. *Mol Pharmacol* **53**, 969–973.

Vlaskovska M, Kasakov L, Rong W, Bodin P, Bardini M, Cockayne DA, Ford AP & Burnstock G (2001). $P2X_3$ knock-out mice reveal a major sensory role for urothelially released ATP. *J Neurosci* **21**, 5670–5677.

Wu G, Whiteside GT, Lee G, Nolan S, Niosi M, Pearson MS & Ilyin VI (2004). A-317491, a selective $P2X_3/P2X_{2/3}$ receptor antagonist, reverses inflammatory mechanical hyperalgesia through action at peripheral receptors in rats. *Eur J Pharmacol* **504**, 45–53.

Wynn G, Rong W, Xiang Z & Burnstock G (2003). Purinergic mechanisms contribute to mechanosensory transduction in the rat colorectum. *Gastroenterology* **125**, 1398–1409.

Zhong Y, Banning AS, Cockayne DA, Ford APDW, Burnstock G & McMahon SB (2003). Bladder and cutaneous sensory neurons of the rat express different functional P2X receptors. *Neuroscience* **120**, 667–675.

Zhong Y, Dunn PM, Bardini M, Ford APDW, Cockayne DA & Burnstock G (2001). Changes in P2X receptor responses of sensory neurons from $P2X_3$-deficient mice. *Eur J Neurosci* **14**, 1784–1792.

Zhong Y, Dunn PM & Burnstock G (2000). Pharmacological comparison of P2X receptors on rat coeliac, mouse coeliac and mouse pelvic ganglion neurons. *Neuropharmacology* **39**, 172–180.

Zhong Y, Dunn PM, Xiang Z, Bo X & Burnstock G (1998). Pharmacological and molecular characterization of P2X receptors in rat pelvic ganglion neurons. *Br J Pharmacol* **125**, 771–781.

Acknowledgements

We thank Amy Berson and Eliza Saclolo for significant contributions in the development and maintenance of the P2X knockout lines described in this study.